Non-axisymmetric equilibrium reconstruction & suppression of density limit disruptions in a current-carrying stellarator

AUBURN UNIVERSITY

CTH Compact Toroidal Hybrid

Princeton Plasma Physics Lab *23 January 2018*

Disruption avoidance and mitigation essential for future tokamak devices

- Disruptions do not routinely occur in stellarators
- Total rotational transform $\iota_{tot} = \iota_{current} + \iota_{vac} = 1/q$

  $\iota_{current}$ from plasma current

  ι_{vac} from external stellarator coils (3D magnetic shaping)
- Small amounts of 3D fields already used tokamaks with $B_{3D}/B_0 \sim 10^{-3}$
  - RWM, ELM control, error field correction

Disruption avoidance and mitigation essential for future tokamak devices

- Disruptions do not routinely occur in stellarators
- Total rotational transform $\iota_{tot} = \iota_{current} + \iota_{vac} = 1/q$

  $\iota_{current}$ from plasma current

  ι_{vac} from external stellarator coils (3D magnetic shaping)
- Small amounts of 3D fields already used tokamaks with $B_{3D}/B_0 \sim 10^{-3}$
  - RWM, ELM control, error field correction
- Question: What is the effect of higher levels of 3D magnetic shaping, $B_{3D}/B_0 \sim 0.1$, on tokamak instabilities and disruptions?

CTH addresses strong 3D shaping effects on MHD instabilities and disruptions

- Stellarator/tokamak hybrid:
  - Ohmic driven current within pre-established stellarator plasma
- Disruption avoidance and improved positional stability observed in earlier hybrid devices[1]

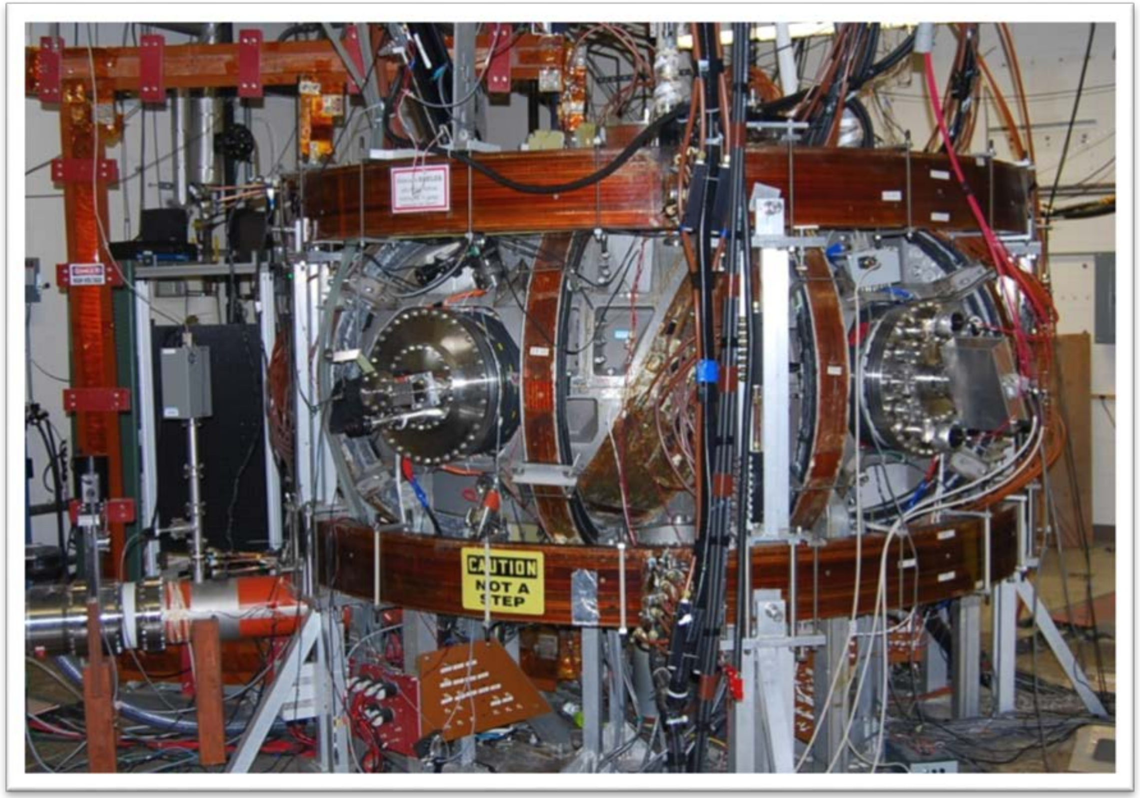

[1] W7-A team, Nucl. Fusion, 1980, H. Ikezi *et al.*,Phys. Fluids, 1979

CTH addresses strong 3D shaping effects on MHD instabilities and disruptions

- Stellarator/tokamak hybrid:
  - Ohmic driven current within pre-established stellarator plasma
- Disruption avoidance and improved positional stability observed in earlier hybrid devices
- Disruptive behavior reproducibly modified by modest levels of vacuum transform

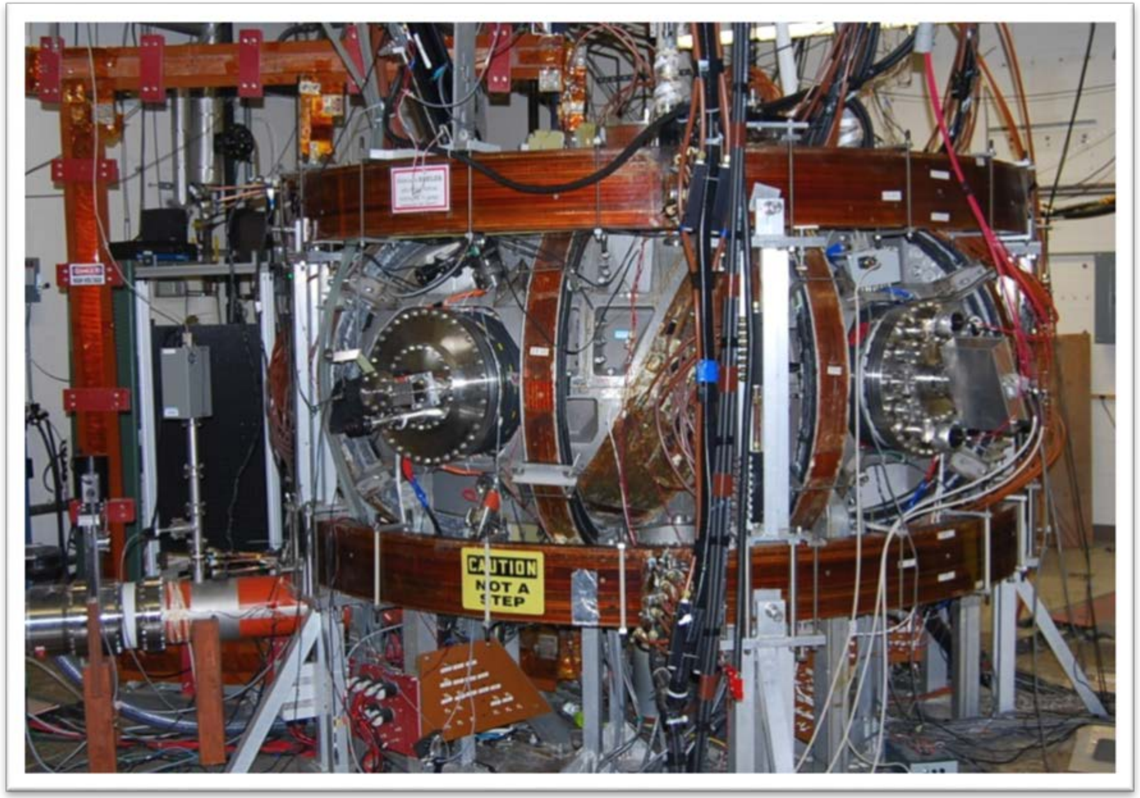

Tokamak operation limited by MHD induced disruptions

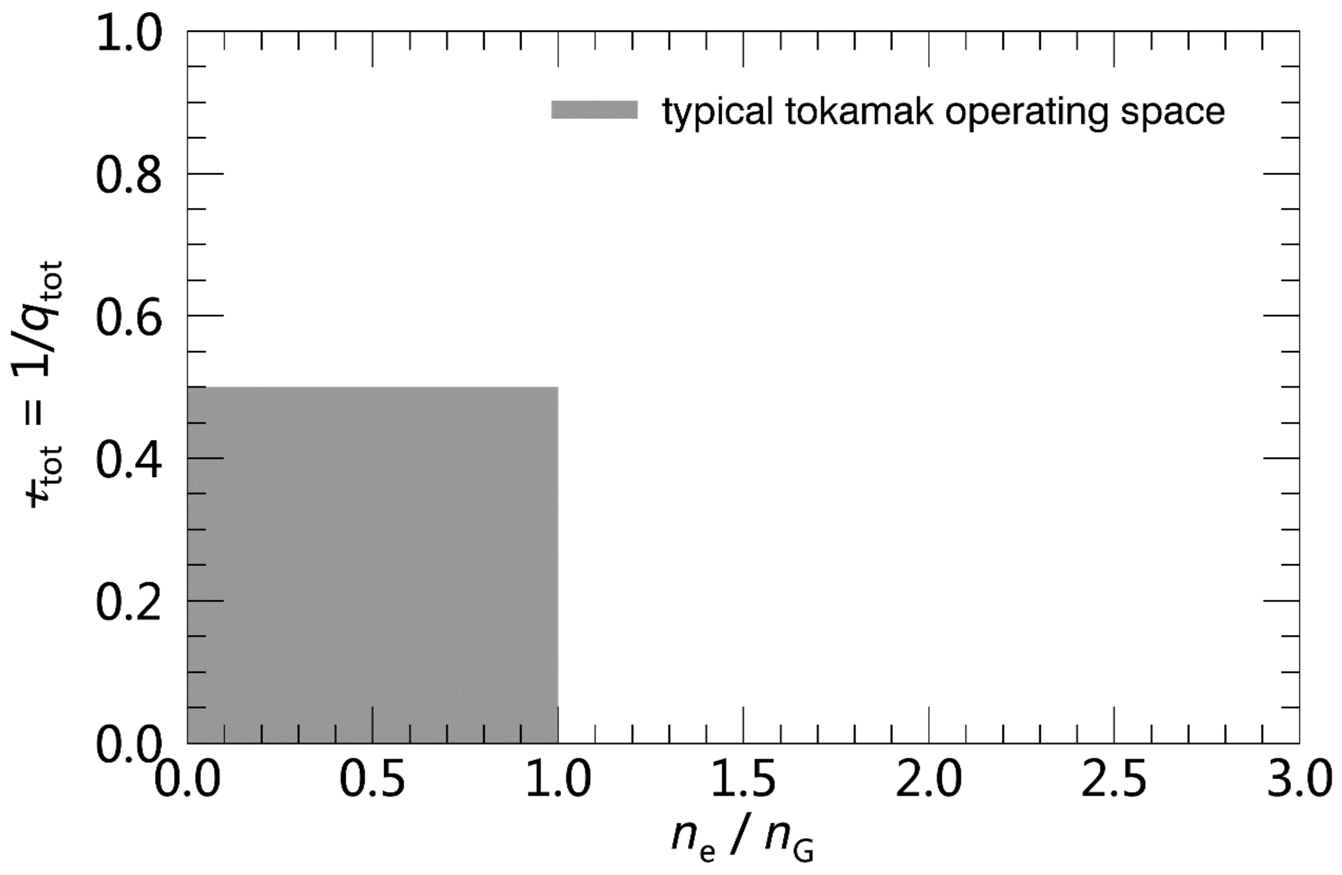

CTH routinely operates beyond the traditional tokamak limits

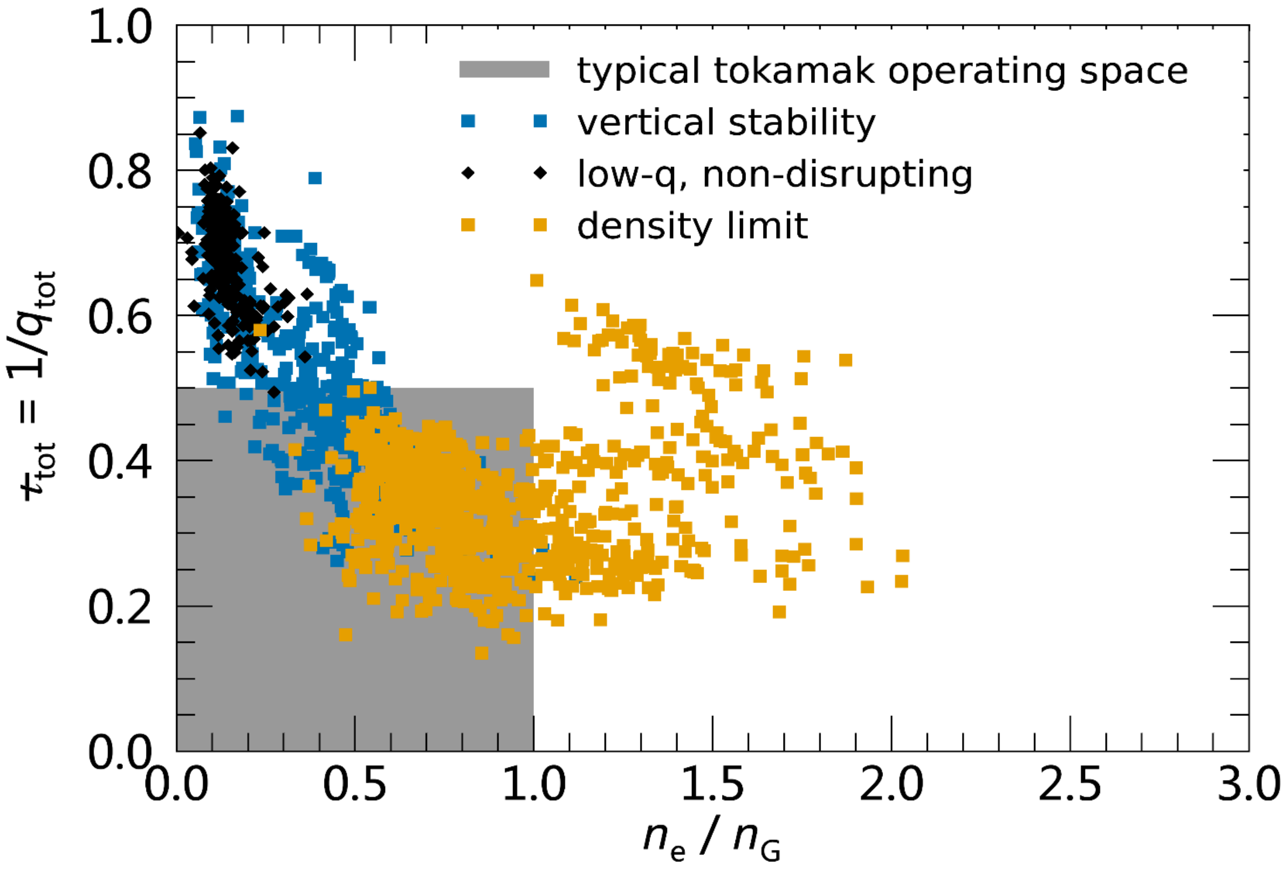

- Vertically stabilized plasmas
- Low-q non-disrupting plasmas
- Disruptive density limit

3D equilibrium reconstruction is an essential tool to understand 3D confinement and stability

- Understanding the intrinsic 3D geometry of stellarator equilibria requires non-axisymmetric three-dimensional equilibrium reconstruction

3D equilibrium reconstruction is an essential tool to understand 3D confinement and stability

- Understanding the intrinsic 3D geometry of stellarator equilibria requires non-axisymmetric three-dimensional equilibrium reconstruction
- CTH is a unique platform to use and benchmark the 3D equilibrium reconstruction code V3FIT[2]
  - Fully 3D equilibrium reconstruction is important to enable study of the effects of strong 3D shaping on instability and disruptions in CTH

[2] J.D. Hanson *et al.*, Nucl. Fusion, 2009

3D equilibrium reconstruction is an essential tool to understand 3D confinement and stability

- Understanding the intrinsic 3D geometry of stellarator equilibria requires non-axisymmetric three-dimensional equilibrium reconstruction
- CTH is a unique platform to use and benchmark the 3D equilibrium reconstruction code V3FIT
  - Fully 3D equilibrium reconstruction is important to enable study of the effect of strong 3D shaping on instability and disruption in CTH
- Nominally axisymmetric plasmas in tokamaks and RFPs can also benefit from 3D equilibrium reconstructions
  - Effects of non-axisymmetric RMP in tokamaks[3]
  - Quasi-helical equilibria in RFPs[4]

[3] S. Lazerson et al., Bulletin of the American Physics Society, 2012
[4] D. Terranova et al., Plasma Physics and Controlled Fusion, 2010

CTH plasmas exhibit strong non-axisymmetric 3D shaping with and without plasma current

$I_p = 0$

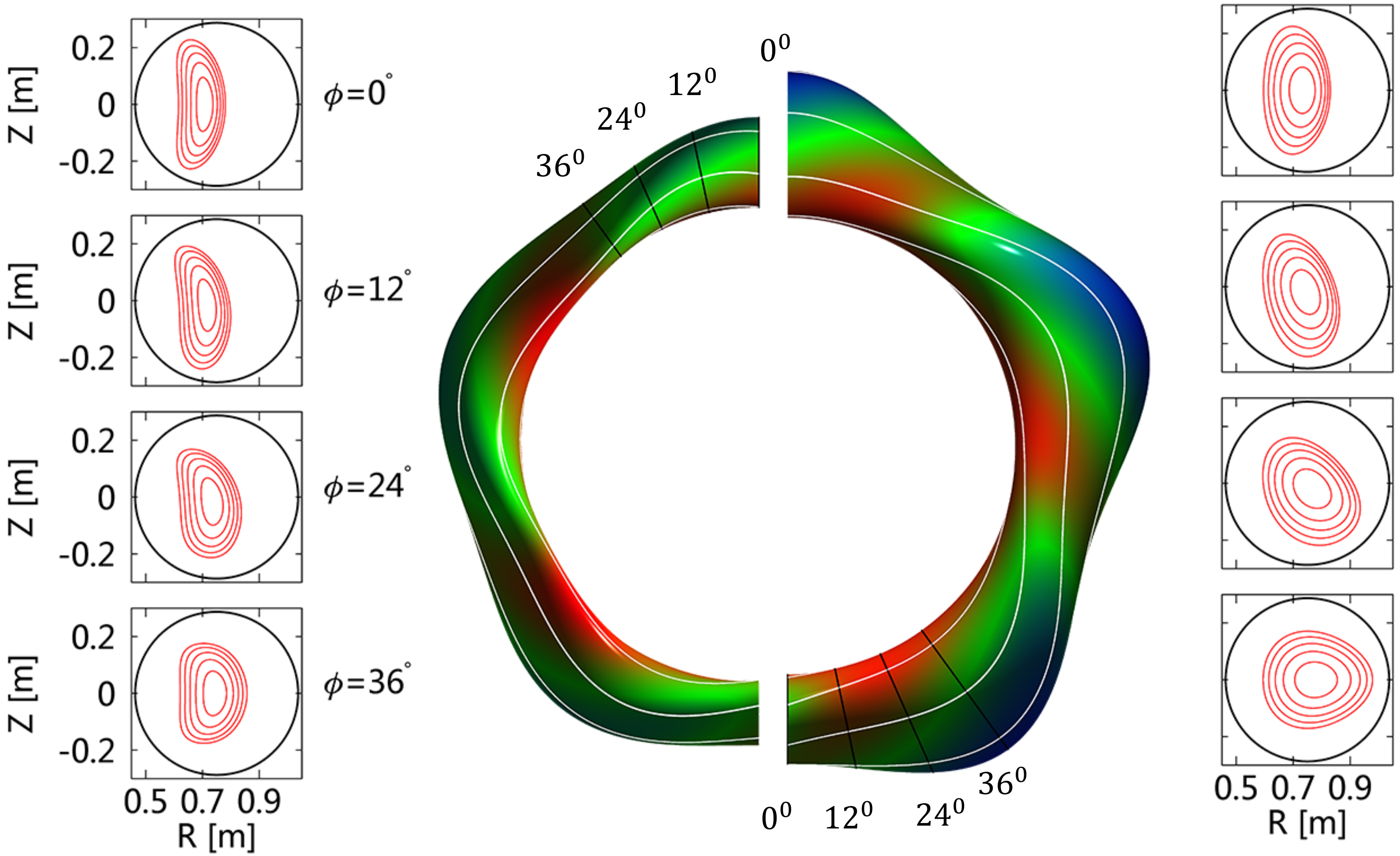

$I_p = 54$ kA

Outline

- Compact Toroidal Hybrid experiment
- VMEC and V3FIT codes
- Improved 3D equilibrium reconstruction with SXR measurements
- Density limit disruption suppression
- Summary

CTH allows flexible vacuum field configurations

- **Helical Field (HF) coil** and **Toroidal Field (TF) coil** currents provide controlled variable vacuum rotational transform

$R_0 = 0.75$ m $R/a \sim 4$ $n_e \leq 5\times10^{19}$ m^{-3} $T_e \leq 150$ eV $|B| \leq 0.7$ T

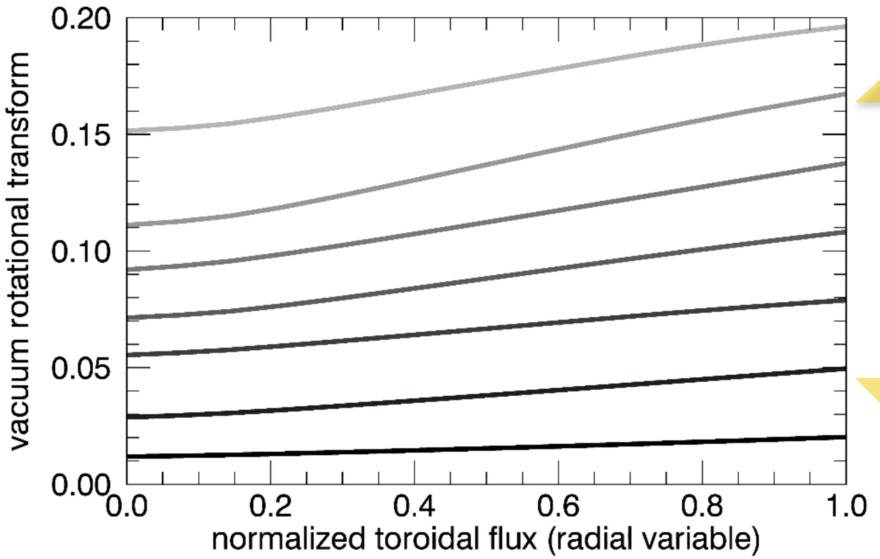

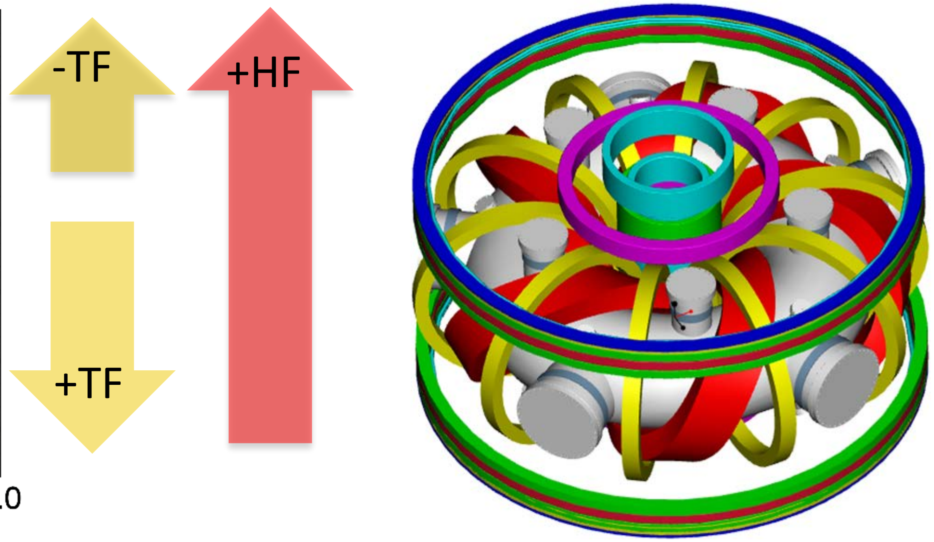

Ohmic coil allows induction of up to 95% of the total rotational transform from plasma current

- **Helical Field (HF) coil** and **Toroidal Field (TF) coil** currents provide controlled variable vacuum rotational transform
- **Central solenoid** drives plasma current, adding to net transform
  - Total rotational transform $\iota_{tot} = \iota_{current} + \iota_{vac}$

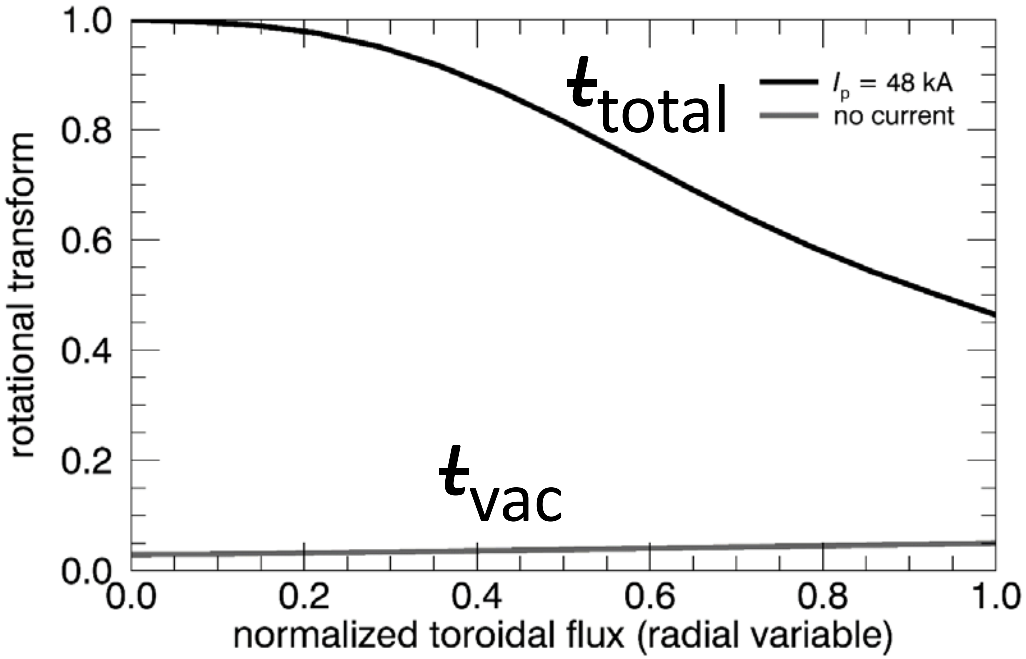

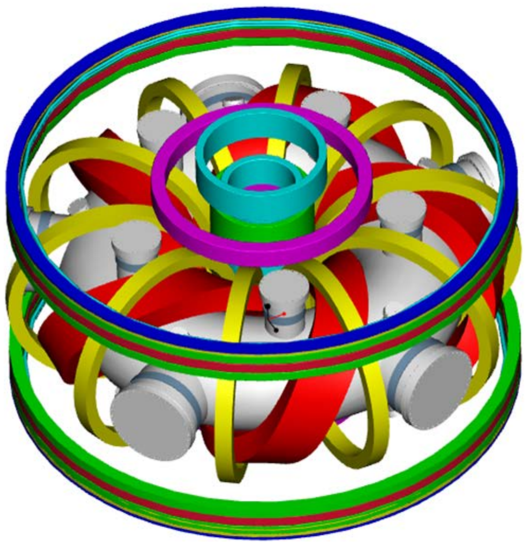

Outline

- Compact Toroidal Hybrid experiment
- VMEC and V3FIT codes
- Improved 3D equilibrium reconstruction with SXR measurements
- Density limit disruption suppression
- Summary

V3FIT uses VMEC as the equilibrium solver to reconstruct CTH plasmas

- VMEC is an ideal MHD 3D equilibrium solver, which solves the MHD force balance equations using variational principle[5]
  - MHD quantities (current and pressure): parameter set $\mathbf{p}$

[5] S.P. Hirshman *et al.*, Comput. Phys. Commun., 1986

V3FIT uses VMEC as the equilibrium solver to reconstruct CTH plasmas

- VMEC is an ideal MHD 3D equilibrium solver, which solves the MHD force balance equations using variational principle[5]
  - MHD quantities (current and pressure): parameter set $\mathbf{p}$
- Using VMEC as the equilibrium solver, V3FIT optimizes the parameter set $\mathbf{p}$ to achieve the best agreement between modeled signals and experimental measurements

$$\chi^2(\mathbf{p}) \equiv \sum_i \left(\frac{S_i^{observed} - S_i^{model}(\mathbf{p})}{\sigma_i} \right)^2$$

  - $S_i^{observed}$ are experimental diagnostic signals
  - S_i^{model} are modeled diagnostic signals calculated by V3FIT
  - σ_i are measurement uncertainties

Outline

- Compact Toroidal Hybrid experiment
- VMEC and V3FIT codes
- Improved 3D equilibrium reconstruction with SXR measurements
- Density limit disruption suppression
- Summary

Numerous magnetic diagnostics designed, installed, calibrated, and incorporated into V3FIT

CTH top view

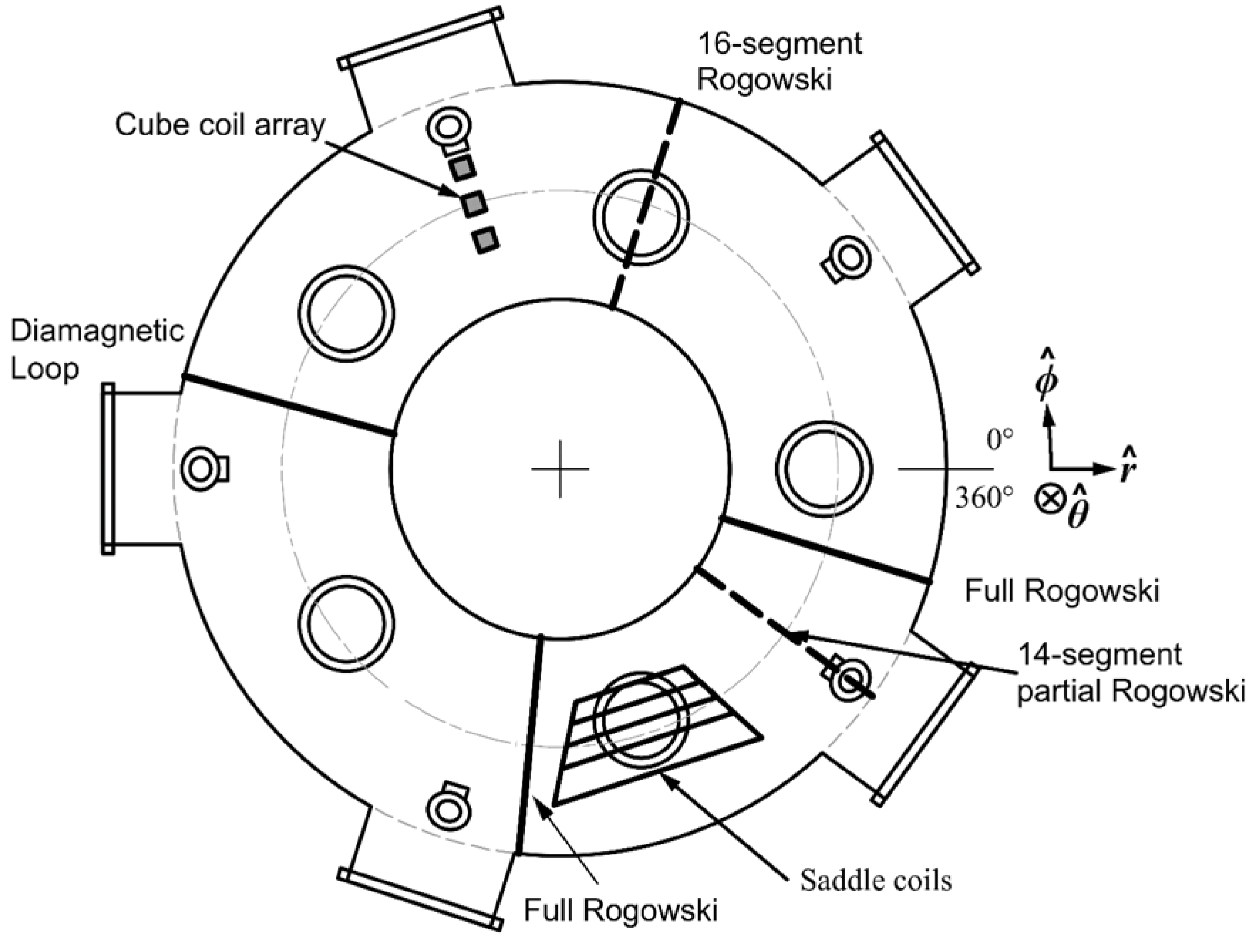

External magnetic diagnostics useful to determine global properties of plasma

- Reconstructions with external magnetic diagnostics give good estimates of edge properties of CTH plasmas
  - Plasma position
  - Plasma shape
  - Edge transform

External magnetic diagnostics useful to determine global properties of plasma

- Reconstructions with external magnetic diagnostics give good estimates of edge properties of CTH plasmas
  - Plasma position
  - Plasma shape
  - Edge transform
- However external magnetics by themselves do not sufficiently describe the internal current distribution

Sawtooth oscillations observed in CTH exhibit behavior similar to that of axisymmetric tokamaks

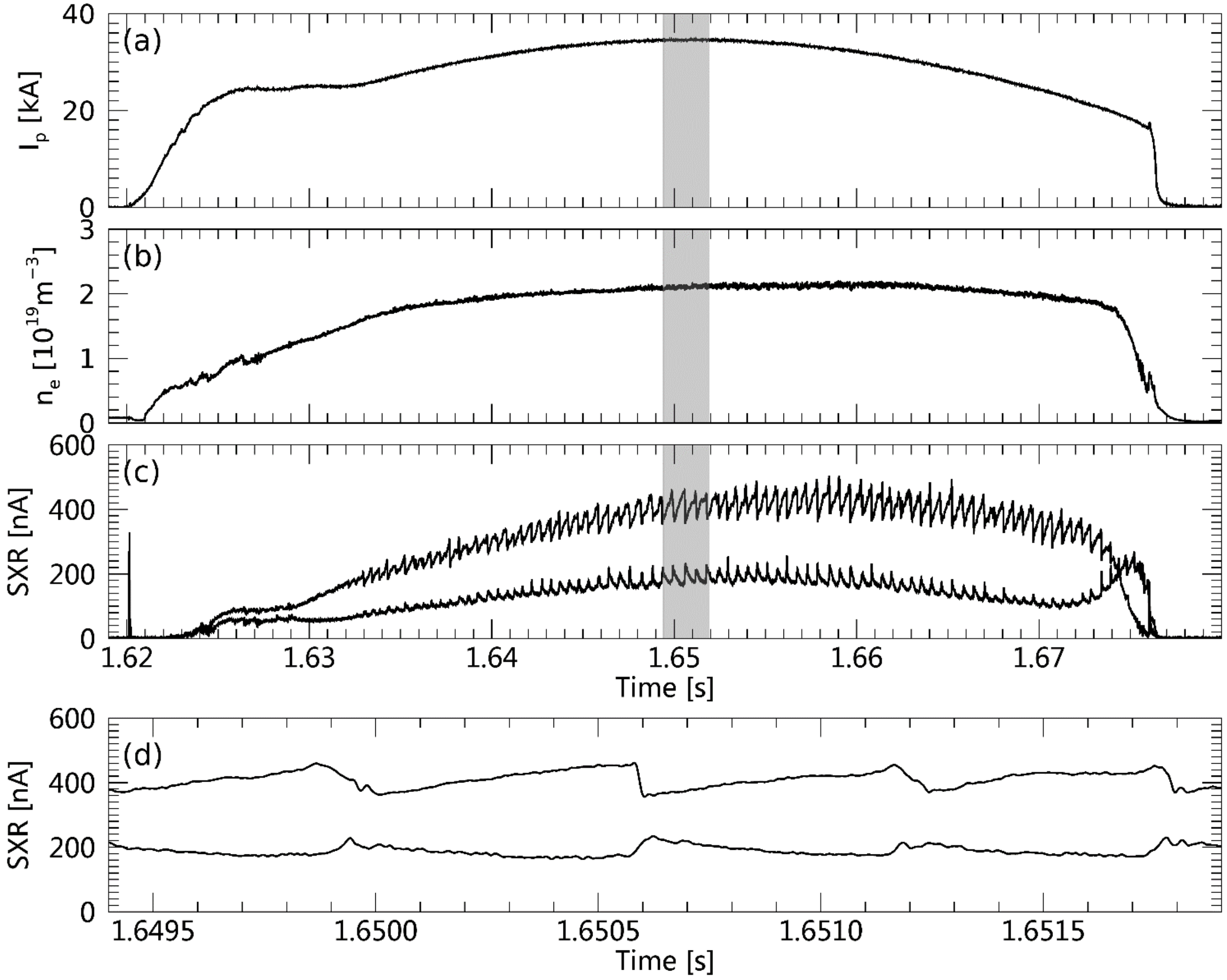

External magnetics alone provide imprecise reconstructions of internal current and q profiles

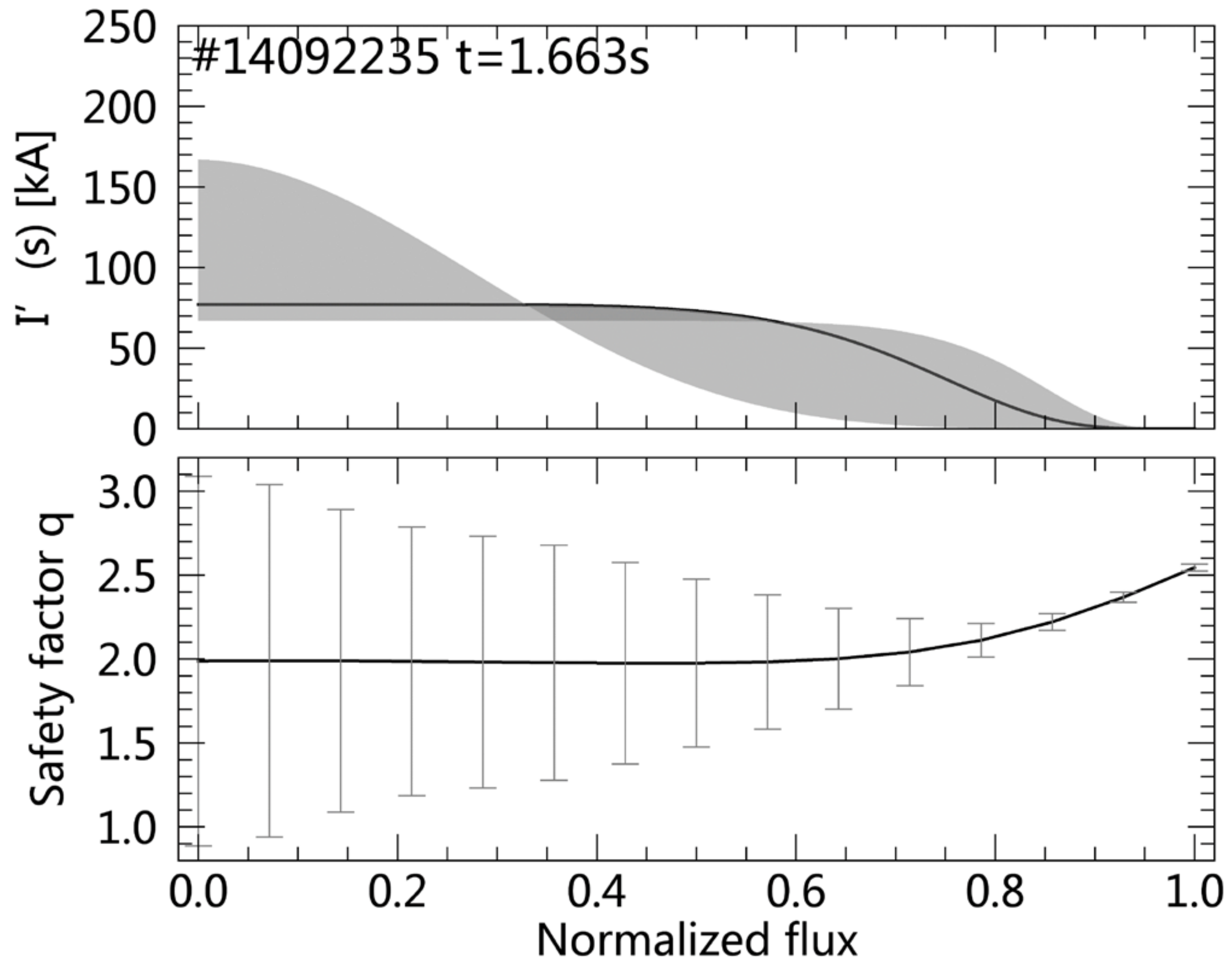

Multiple SXR cameras installed on CTH

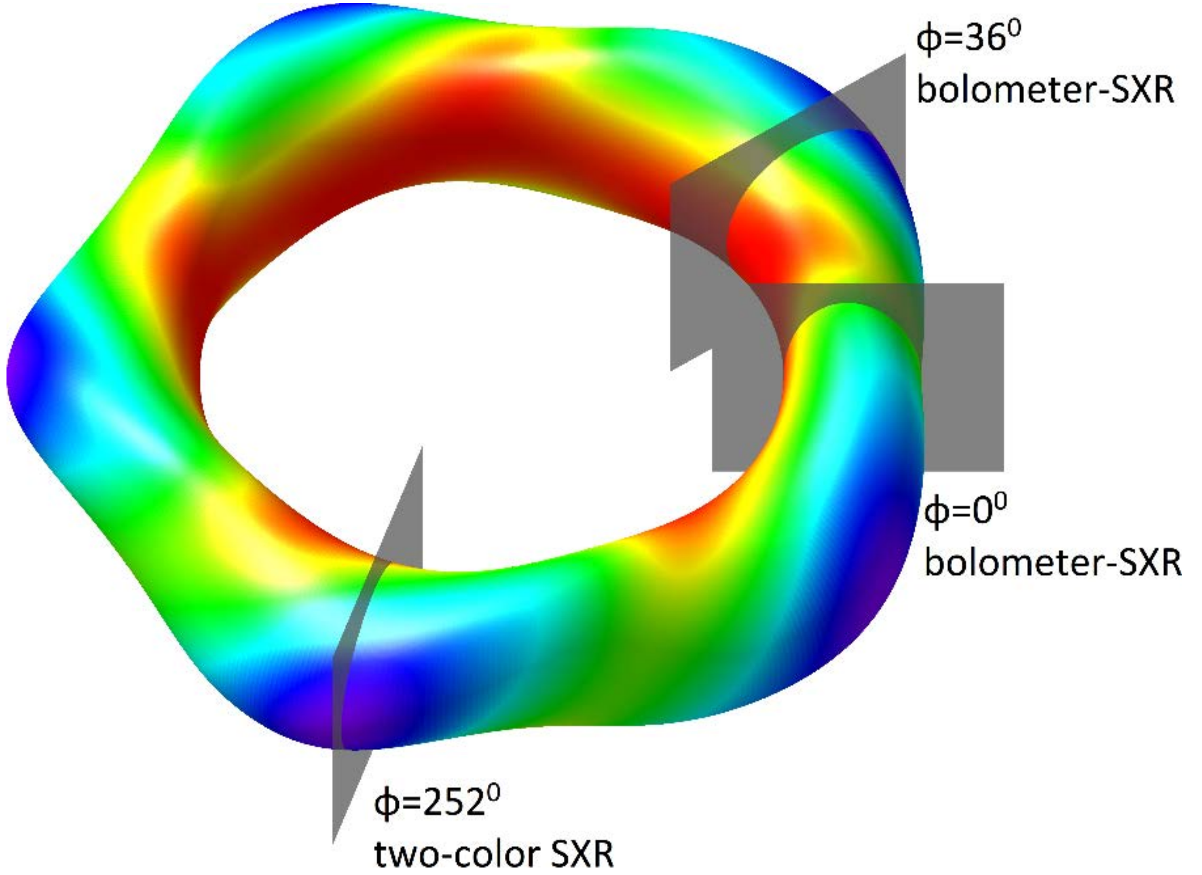

[7] J.L. Herfindal *et al.*, RSI, Vol.85, No.11, 2014

Two different methods have been developed to incorporate SXR measurements in V3FIT

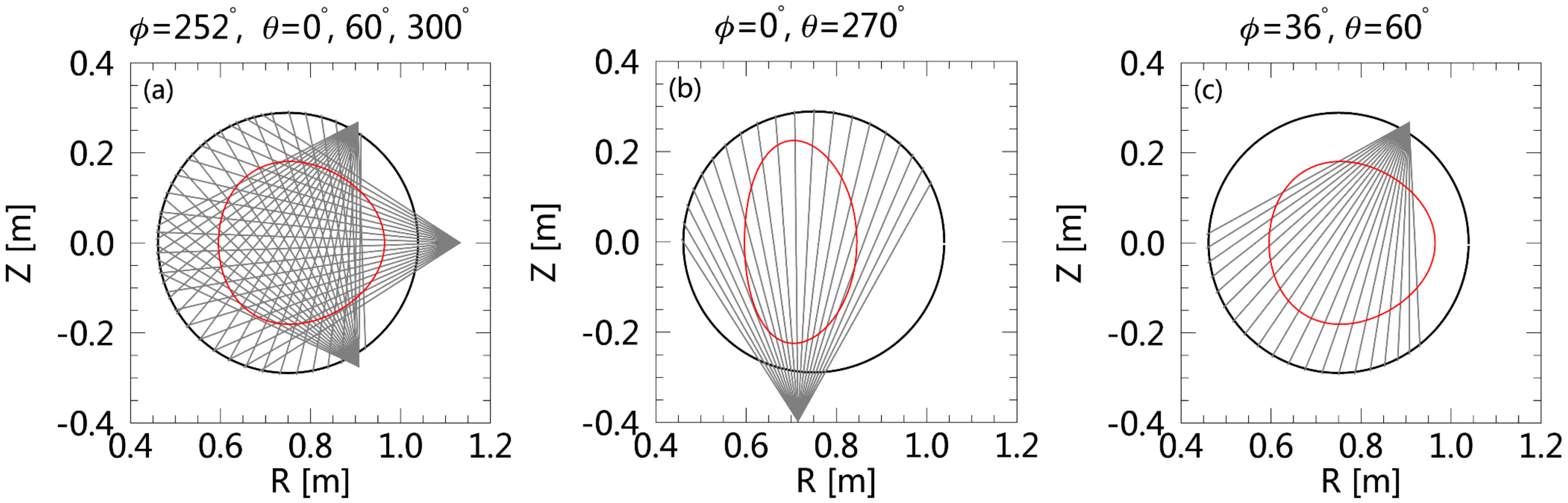

1. Sawtooth inversion radius is used to locate the q=1 surface[8]
2. SXR emissivity profiles reconstructed using all 160 signals[9]

[8] X. Ma et al., Physics of Plasmas, 2015
[9] X. Ma et al., submitted to Physics of Plasmas, 2017

Reconstructed Bi-orthogonal Decomposition signals identify sawtooth inversion radius location

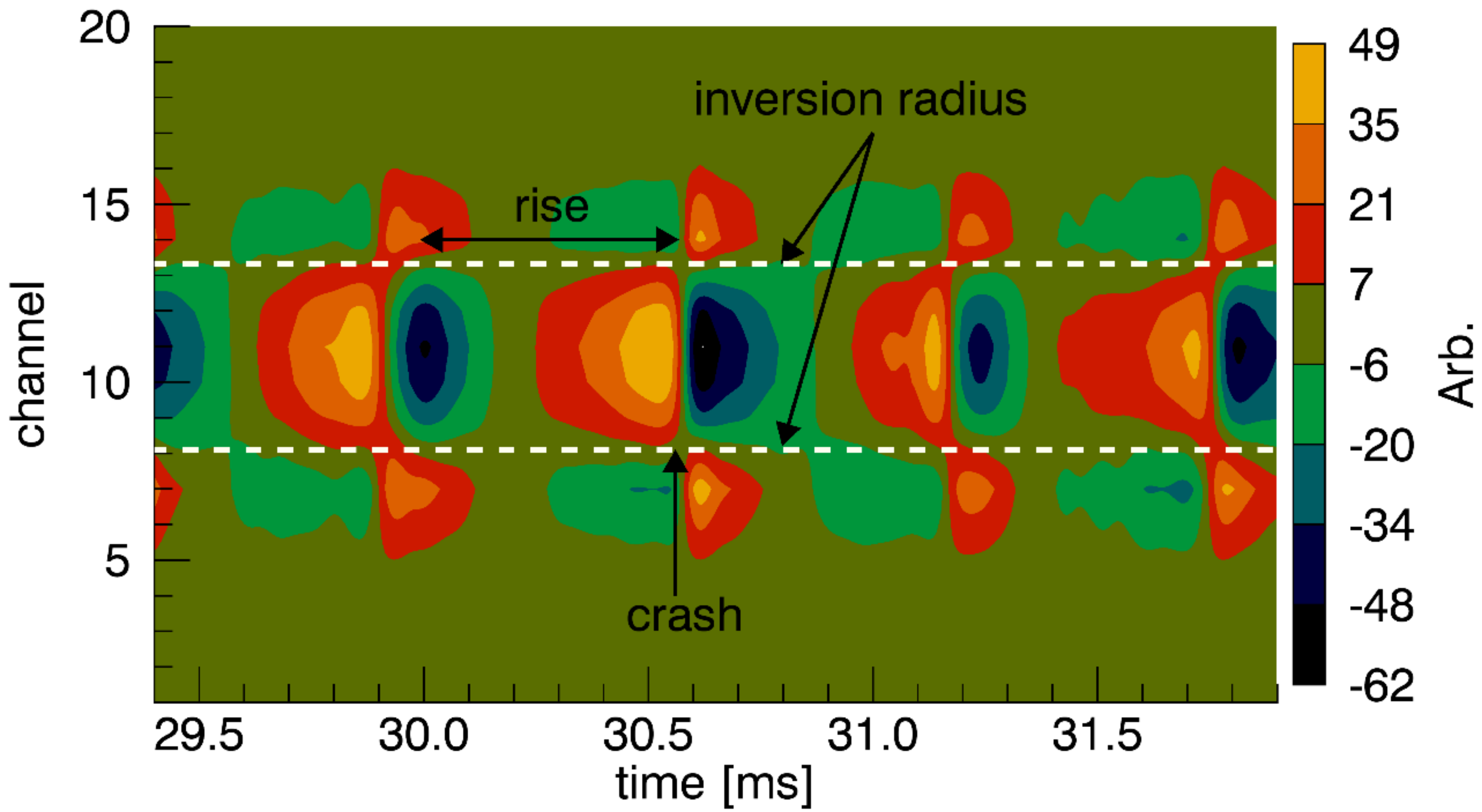

- Reconstructed SXR signals using the first two modes of Bi-orthogonal Decomposition (BD)

Inversion surface used to map the positon of q=1 surface to flux space

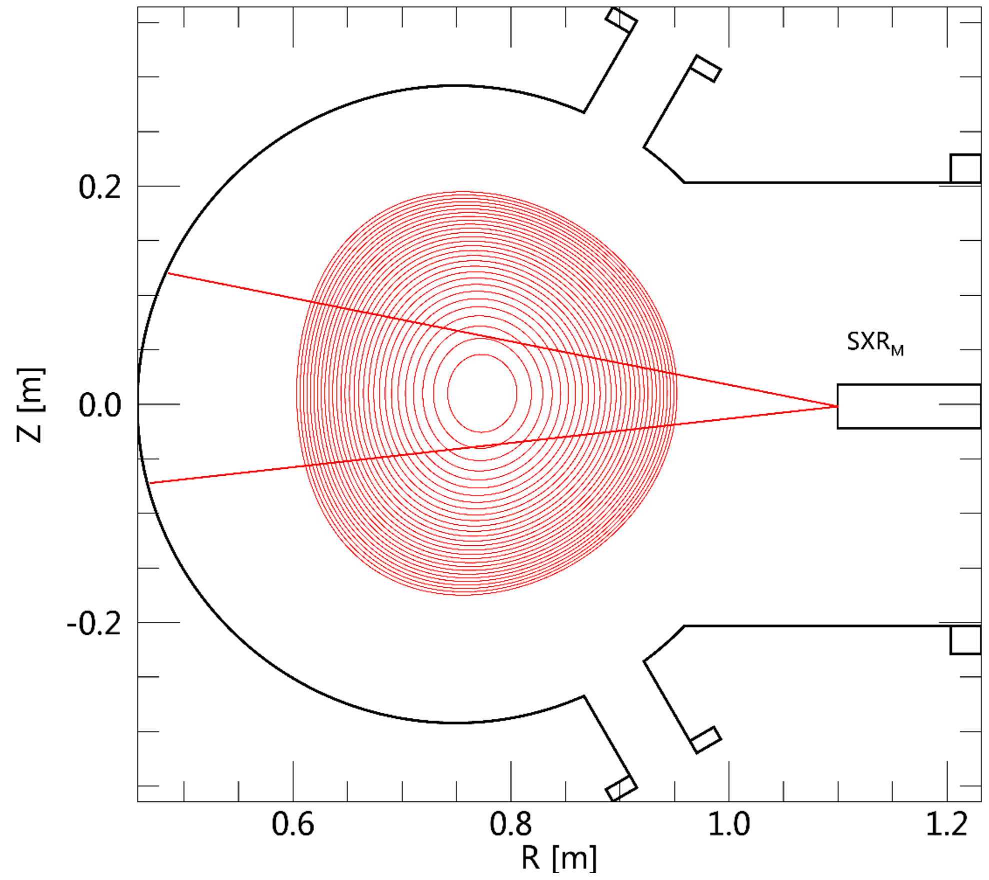

- q=1 surface information used as a constraint in V3FIT

Two different methods have been developed to incorporate SXR measurements in V3FIT

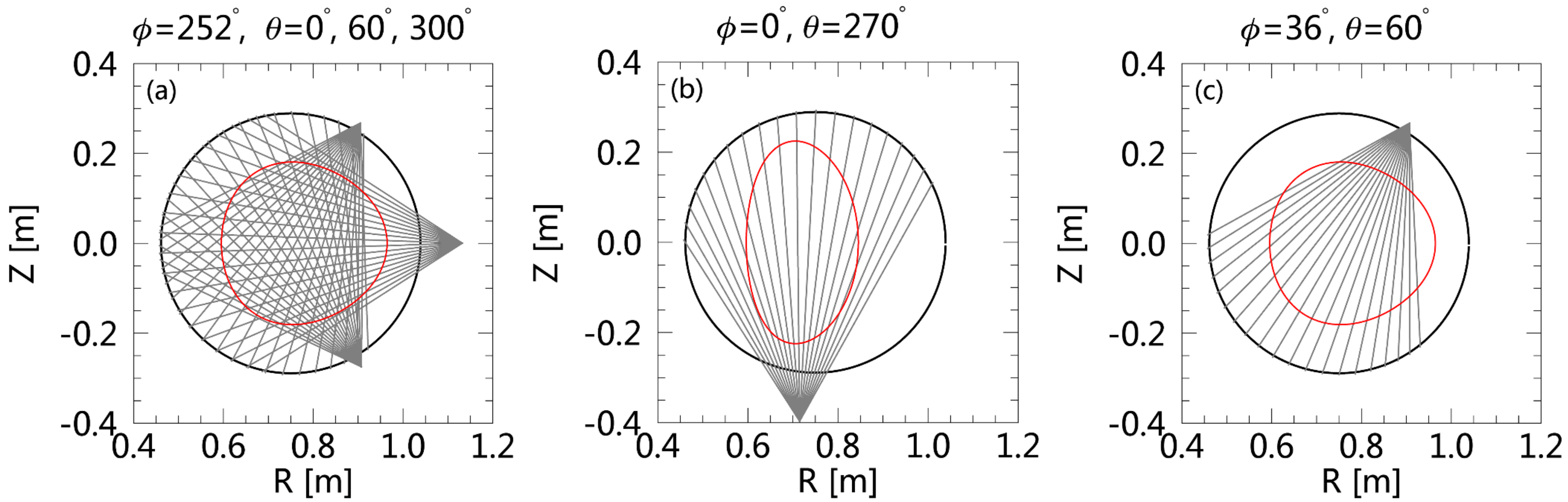

1. Sawtooth inversion radius is used to locate the q=1 surface
2. SXR emissivity profiles reconstructed using all 160 signals

Current distribution determined from geometry of magnetic flux surfaces[10]

- SXR diagnostic has been used to infer current and q profiles in JET[11] and PEGASUS[12]
  - Only works for non-circular plasmas
  - Multiple-step implementation

[10] J. Christiansen and J. Taylor, Nuclear Fusion, 1982
[11] J. Christiansen et al., Nuclear Fusion, 1989
[12] K. Tritz et al., Review of Science Instruments, 2003

SXR data directly incorporated in V3FIT to reconstruct emissivity profiles

- SXR emission assumed to be a flux surface quantity
  - Electron density, temperature and impurity concentration assumed to be constant on flux surfaces
- SXR measurements treated as line-integrated signals
- Reconstructed emissivity profiles constrain the shape of flux surfaces and current distribution

SXR Signals
+
Geometric information

→

Reconstructed emissivity profiles

Modeled emissivity signals in good agreement with experimental measurements

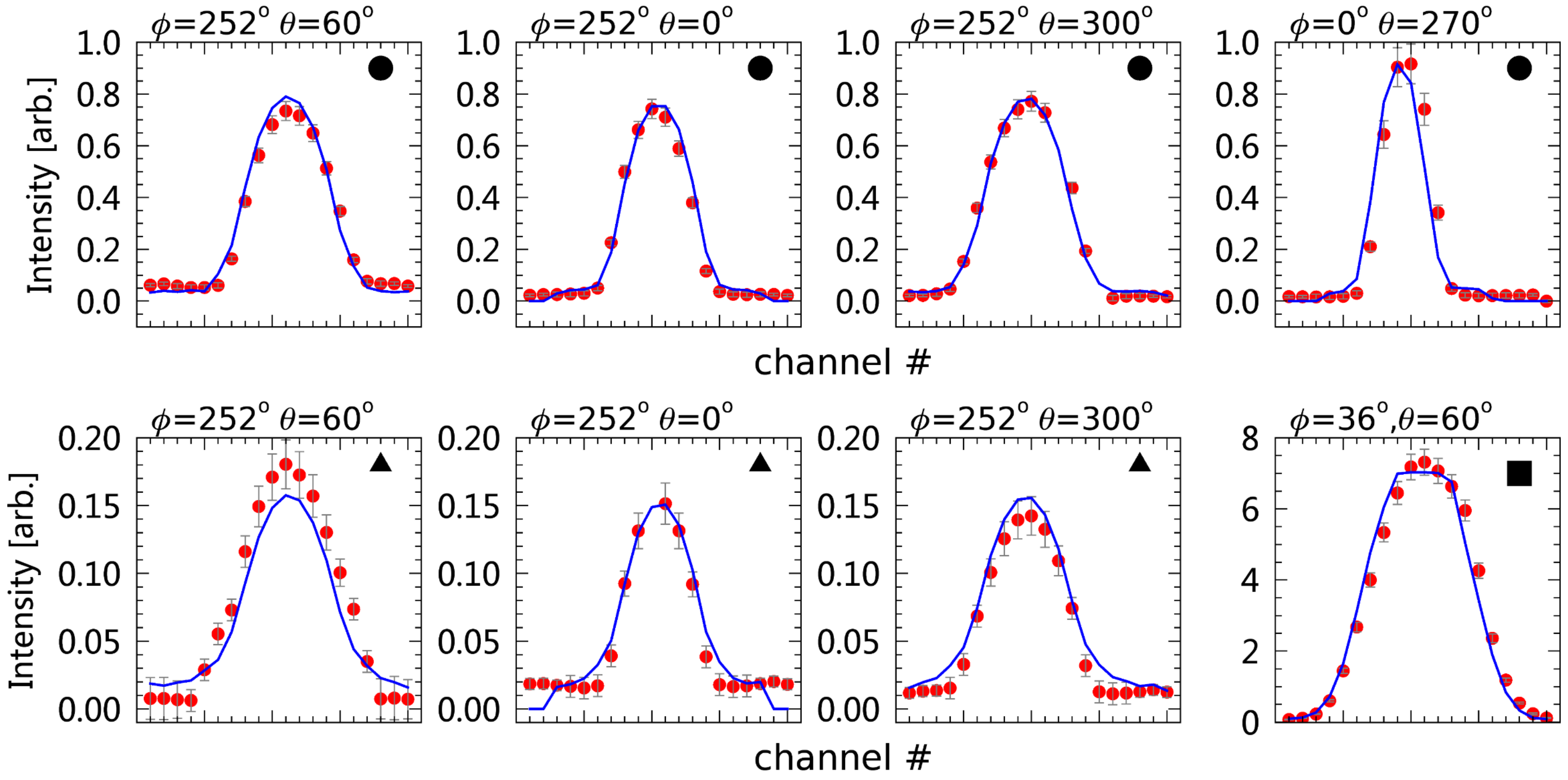

Inclusion of SXR information channels more current in the plasma core

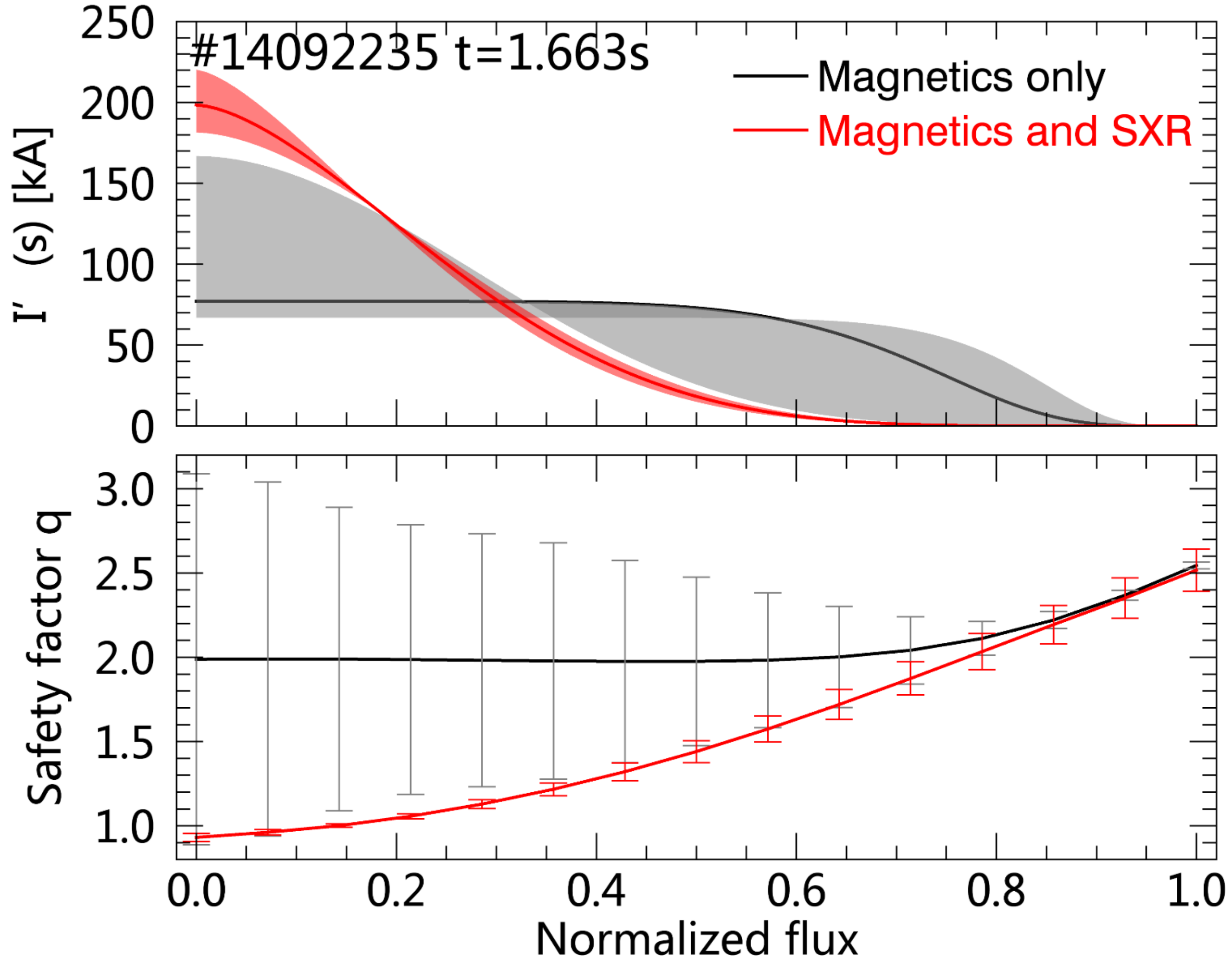

Reconstructed q_0 using SXR data in good agreement with using the q=1 constraint from inversion radius

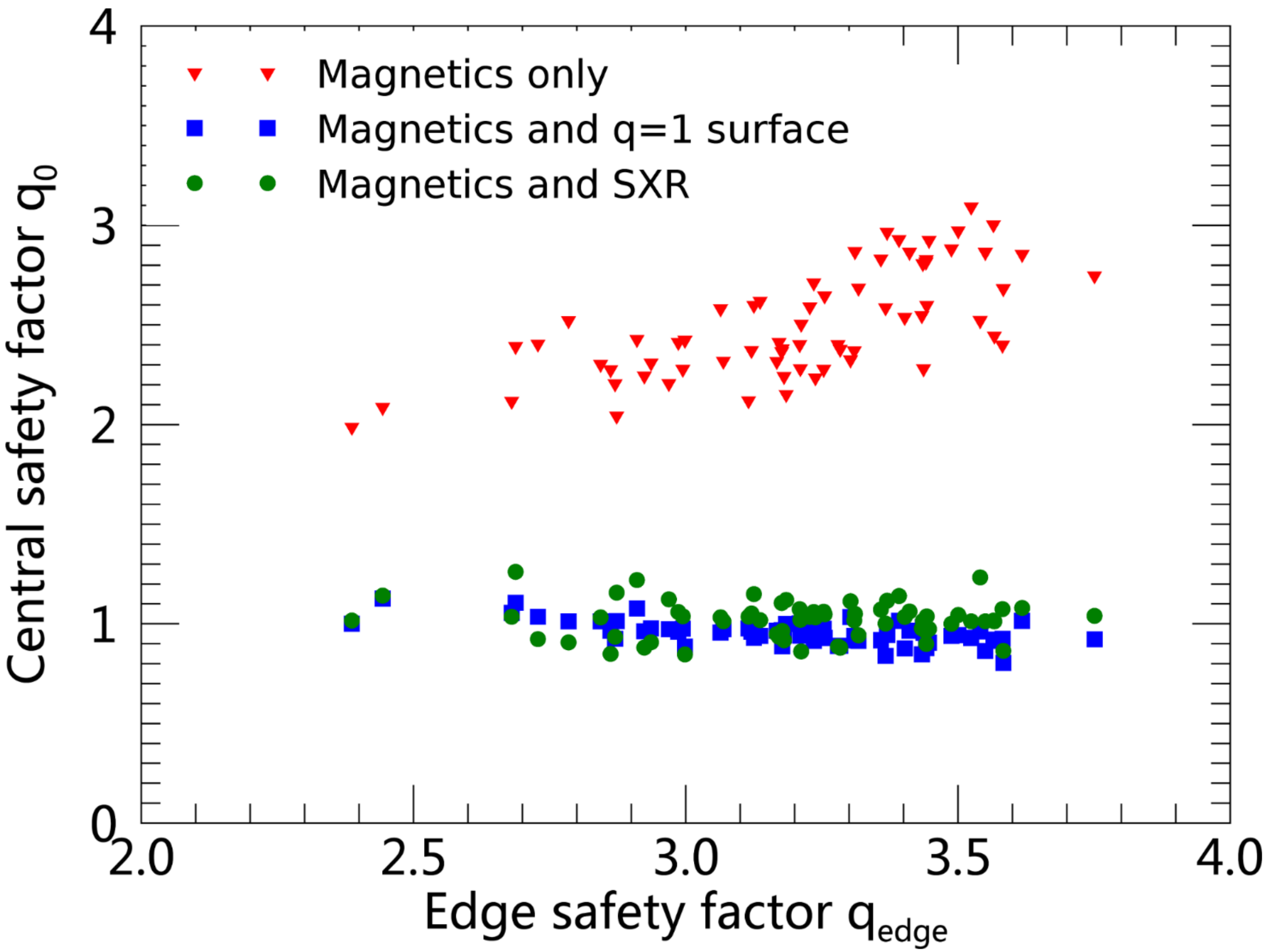

Group of discharges with similar current, density and varying external vacuum transform

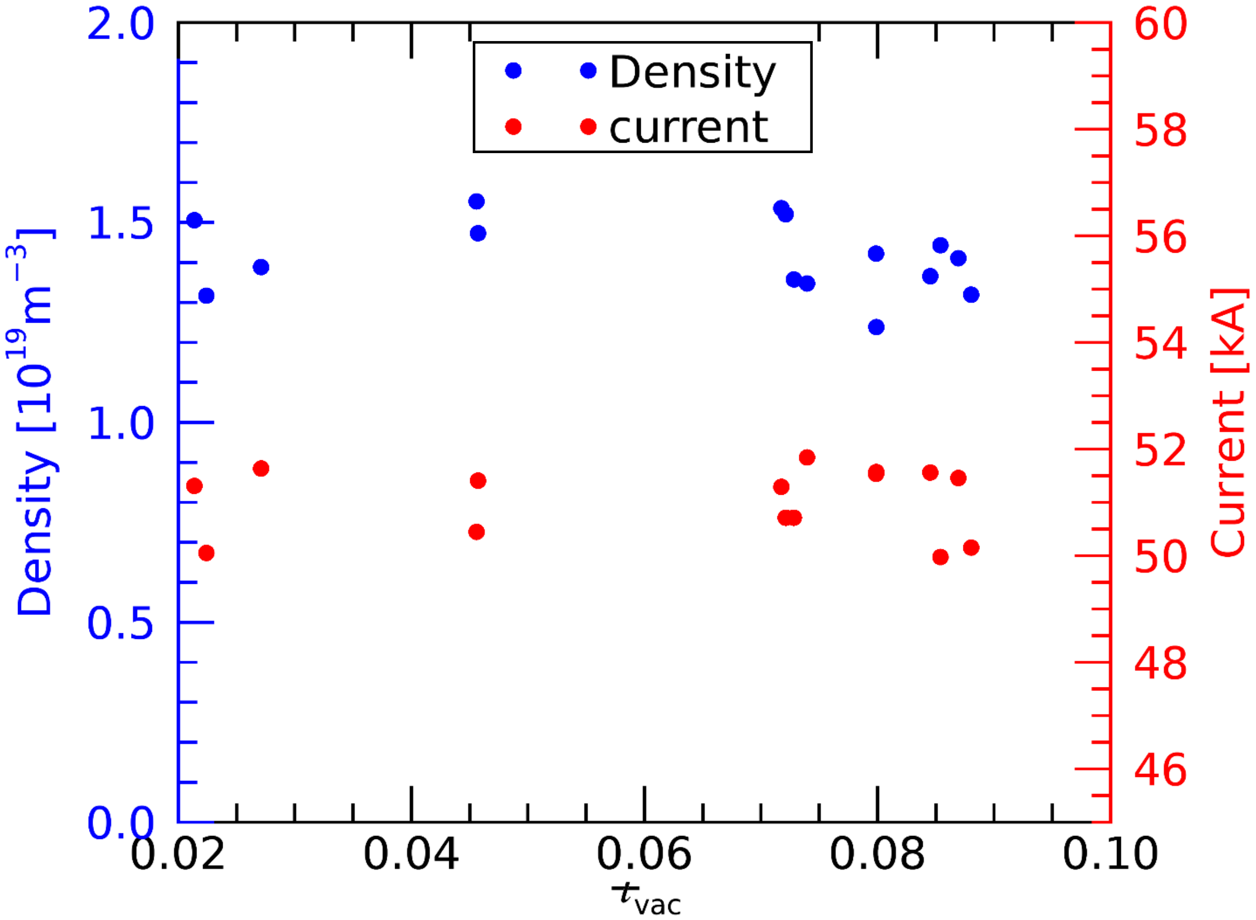

Addition of external 3D fields broadens current profile

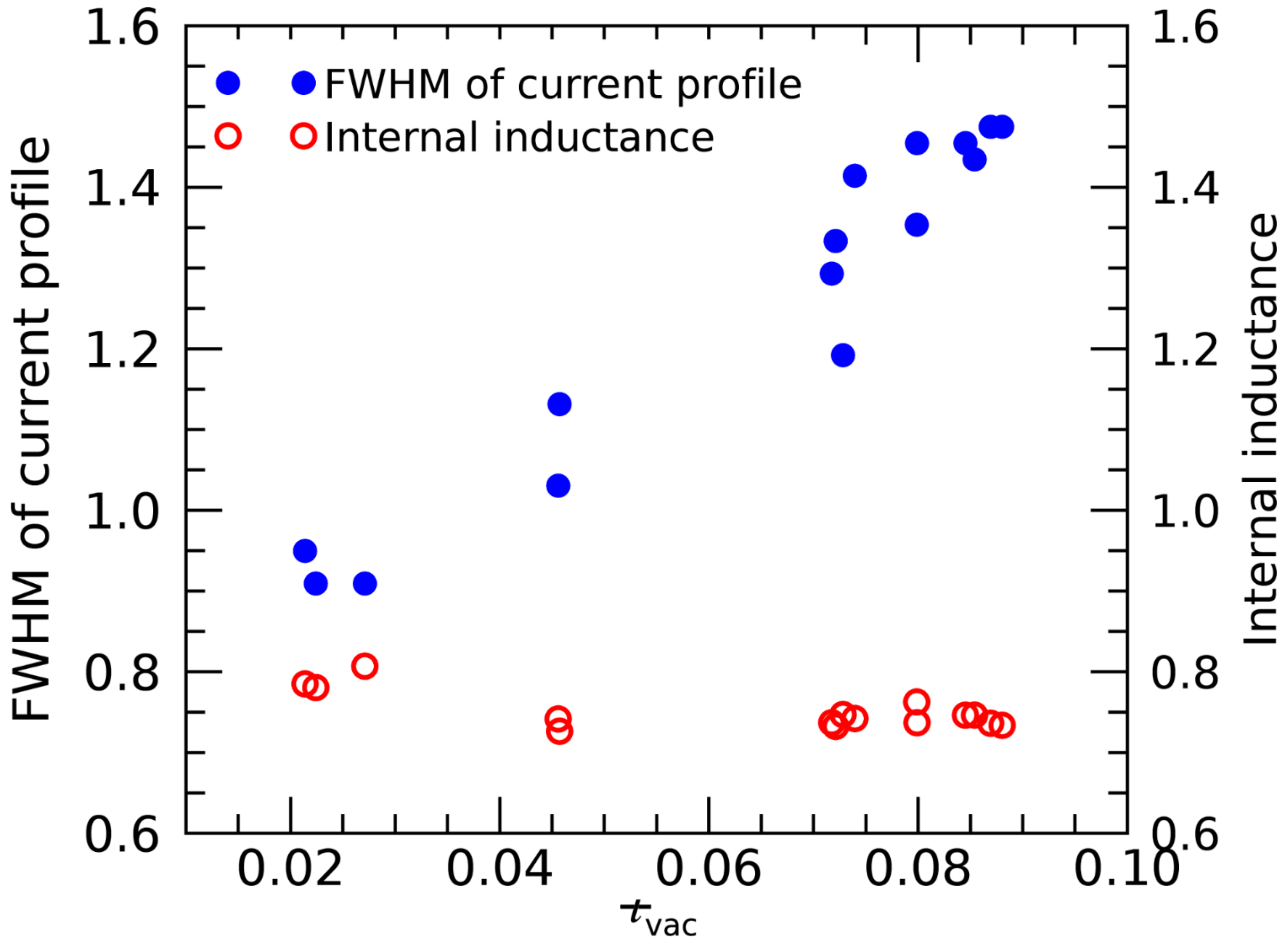

Outline

- Compact Toroidal Hybrid experiment
- VMEC and V3FIT codes
- Improved 3D equilibrium reconstruction with SXR measurements
- Density limit disruption suppression
- Summary

The tokamak density limit

- Empirically determined Greenwald limit[13]

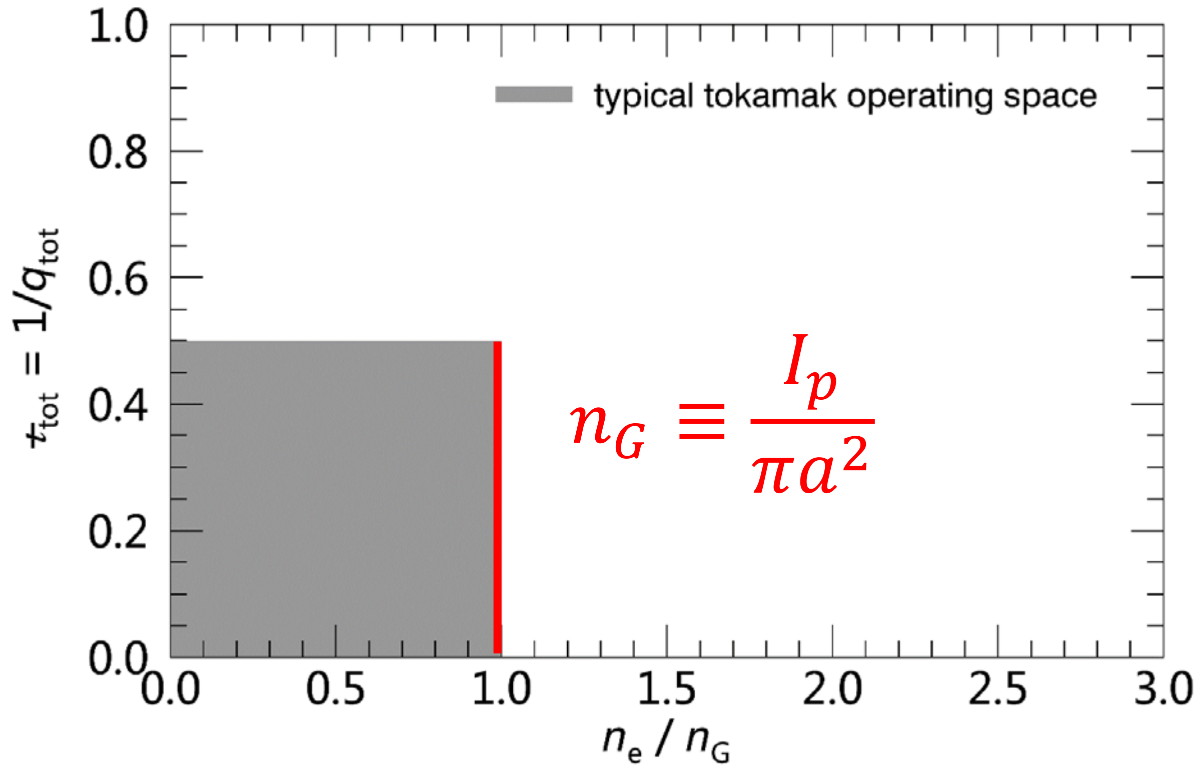

[13] M. Greenwald *et al.,* Nucl. Fusion, 1988

Present understanding of the tokamak density limit

- Empirically determined Greenwald limit
- High density operation induces cooling of edge plasma and current profile contraction giving rise to MHD instability and disruption

Present understanding of the tokamak density limit

- Empirically determined Greenwald limit
- High density operation induces cooling of edge plasma and current profile contraction giving rise to MHD instability and disruption
- No widely accepted first principles theory, not even agreement on critical physics[14]

[14] M. Greenwald, Plasma Phys. Control. Fusion, 2002

Present understanding of the tokamak density limit

- Empirically determined Greenwald limit
- High density operation induces cooling of edge plasma and current profile contraction giving rise to MHD instability and disruption
- No widely accepted first principles theory, not even agreement on critical physics
- Some possible candidates:
  - Increased transport at high density
  - Global radiative instability
  - Thermally unstable magnetic islands

Present understanding of the tokamak density limit

- Empirically determined Greenwald limit
- High density operation induces cooling of edge plasma and current profile contraction giving rise to MHD instability and disruption
- No widely accepted first principles theory, not even agreement on critical physics
- Some possible candidates:
  - Increased transport at high density
  - Global radiative instability
  - Thermally unstable magnetic islands
- General agreement on final scenario:

Current profile shrinkage → MHD instability → disruption

3D shaping with stellarator fields modifies the observed density limit in CTH

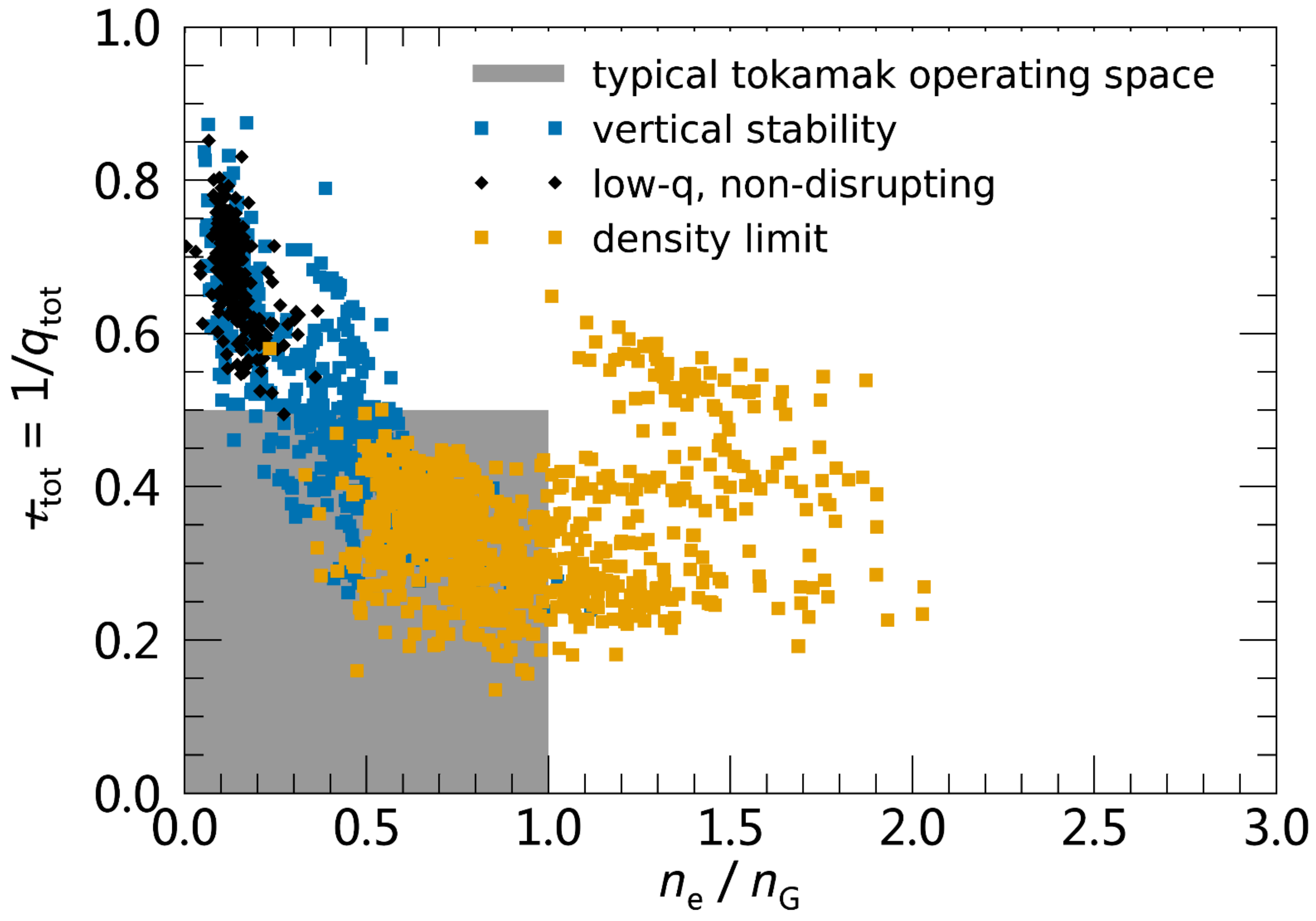

Density limit disruption can be triggered by edge fueling

- The high density shot disrupted with ramping density
- Phenomenology of terminations similar to tokamak disruptions
- Disruption occurrence correlates with plasma current and density

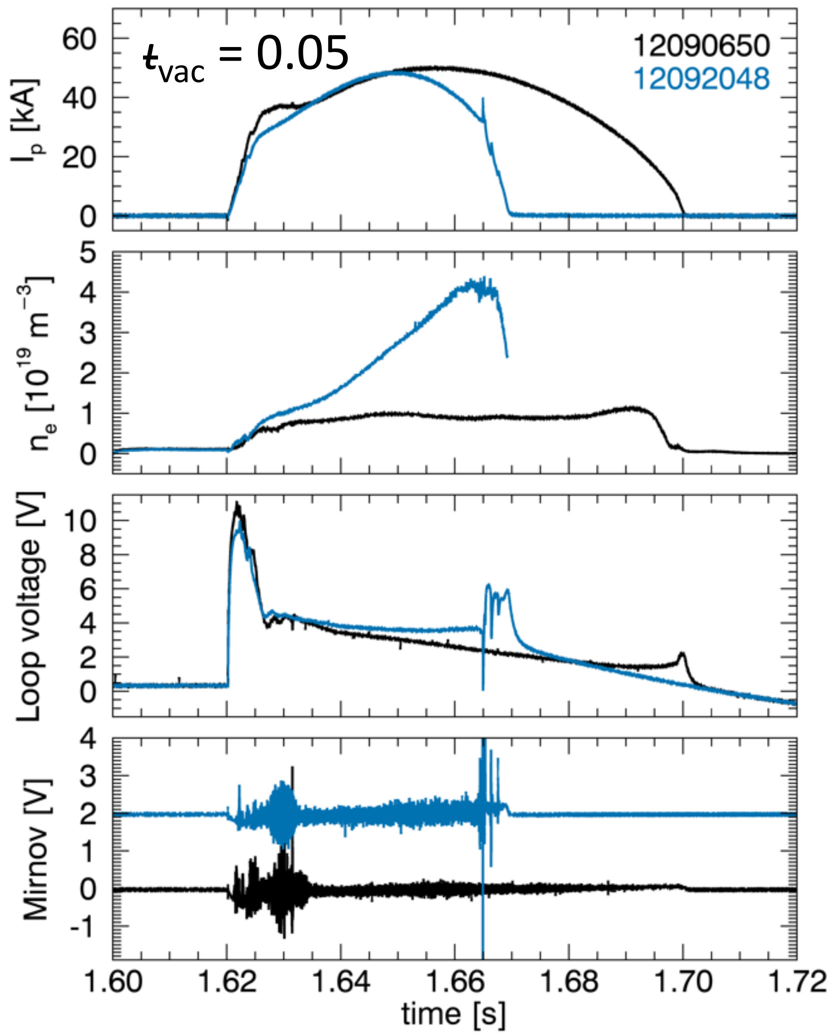

Growing fluctuations observed prior to disruption on multiple signals

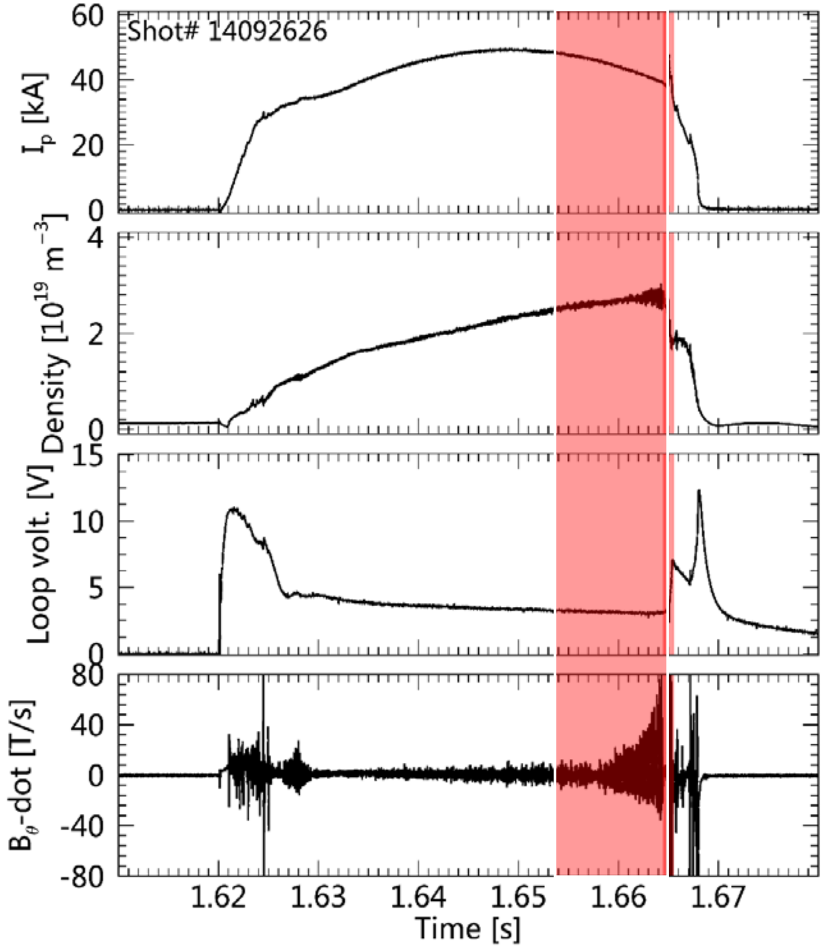

- MHD modulates density and SXR emission

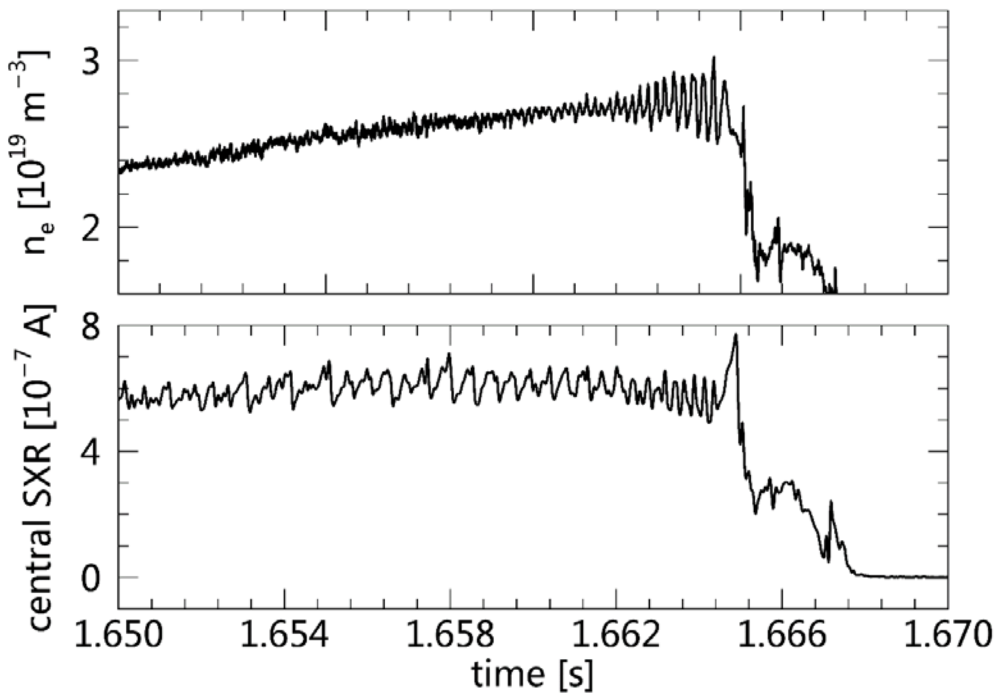

m/n = 2/1 mode identified prior to disruption

poloidal array of B_θ probes

m=2

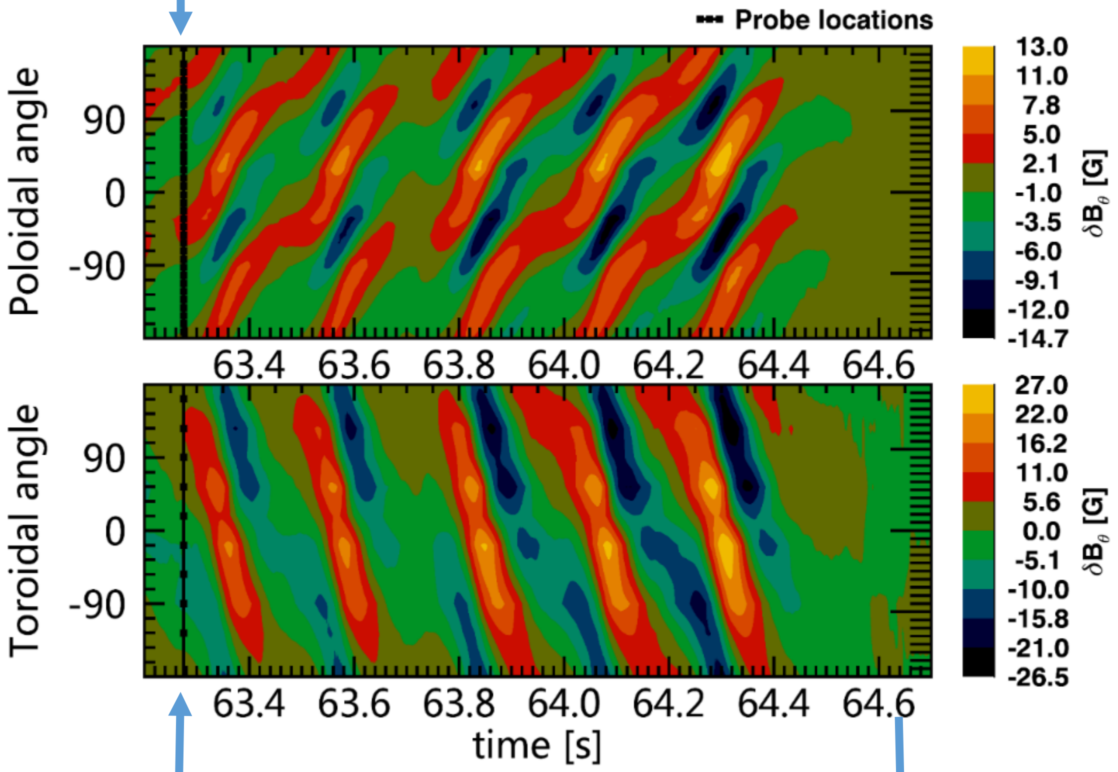

toroidal array of B_θ probes

n=1

Disruption

Growing 2/1 mode

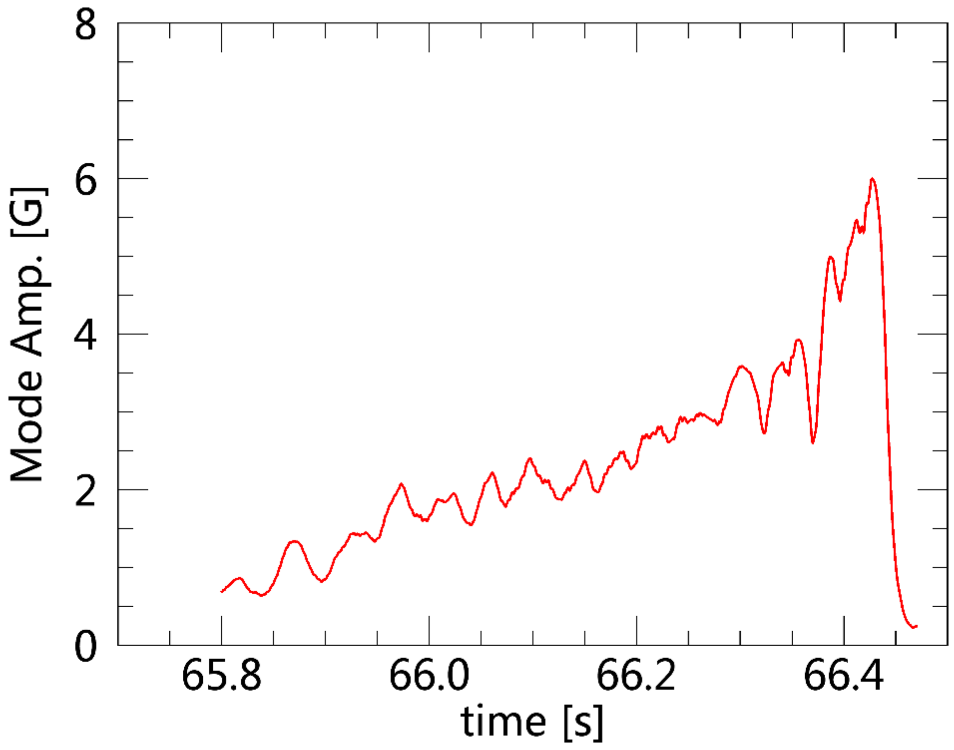

Time evolution of reconstructions show sudden narrowing of current profile before disruption

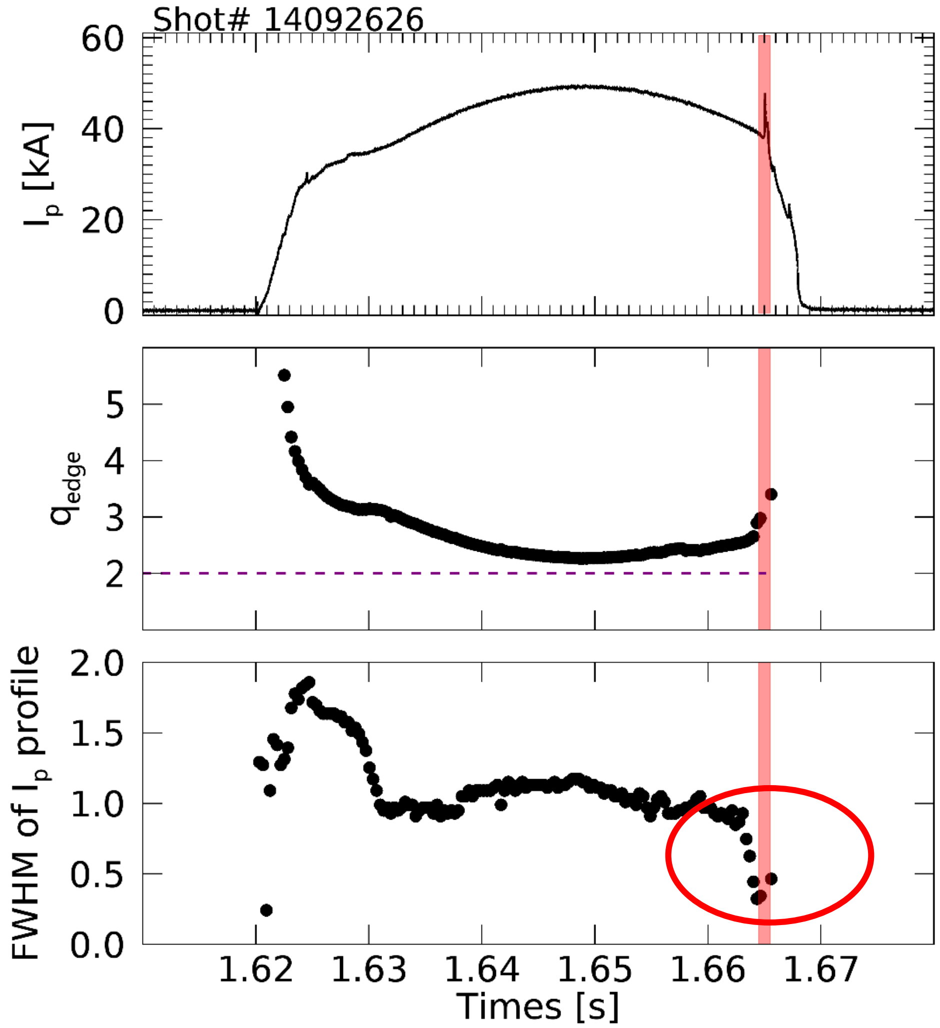

- $q = 2$ surface moves towards plasma core before disruption
- Peaking of current profile leads to steeper current gradient at $q = 2$
    - Plasma is MHD unstable to growing 2/1 mode

Addition of vacuum transform delays disruption

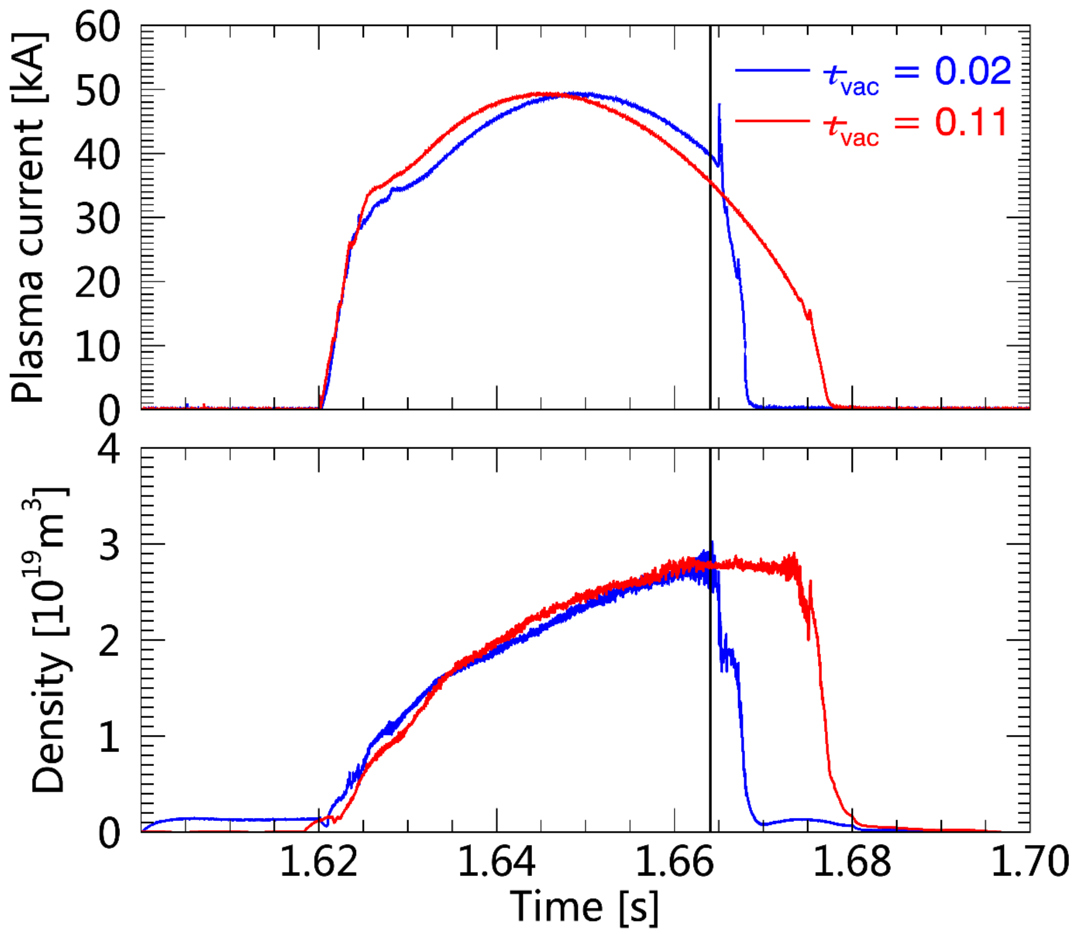

- Two discharges ended in density limit disruptions
- Similar current and density traces up to the point where the blue shot (with low vacuum transform) disrupted early

Flattened current and q profiles with additional 3D fields

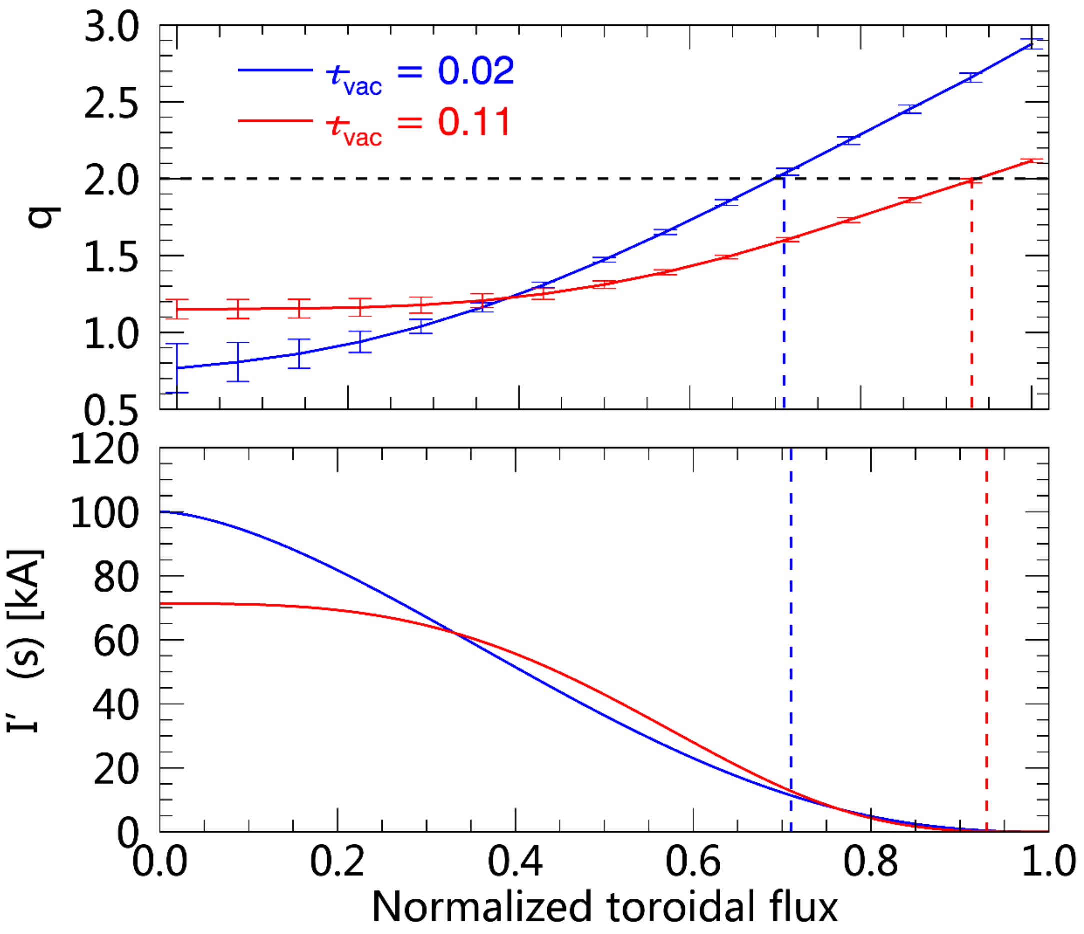

- Reconstructions done at the same time before blue shot disrupted
- Additional vacuum transform moves the q=2 surface to the edge
- Steeper gradient in current profile at q=2 for low vacuum discharge

For a given current, higher densities achieved with addition of vacuum transform

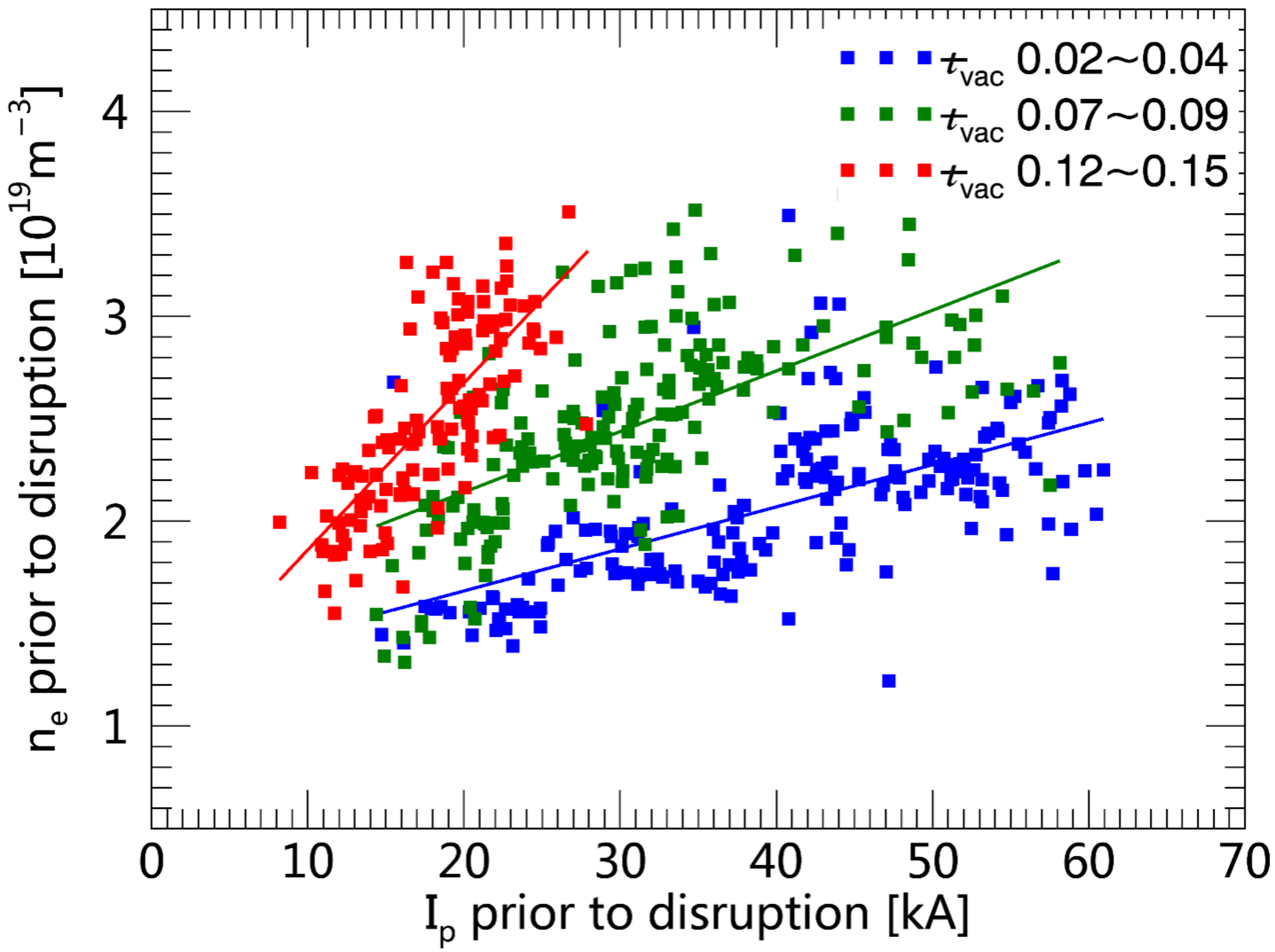

- Density before disruption scales with current
- Additional dependence on applied vacuum transform

Normalized density limit increases by a factor of 3 to 4 as the vacuum transform is raised

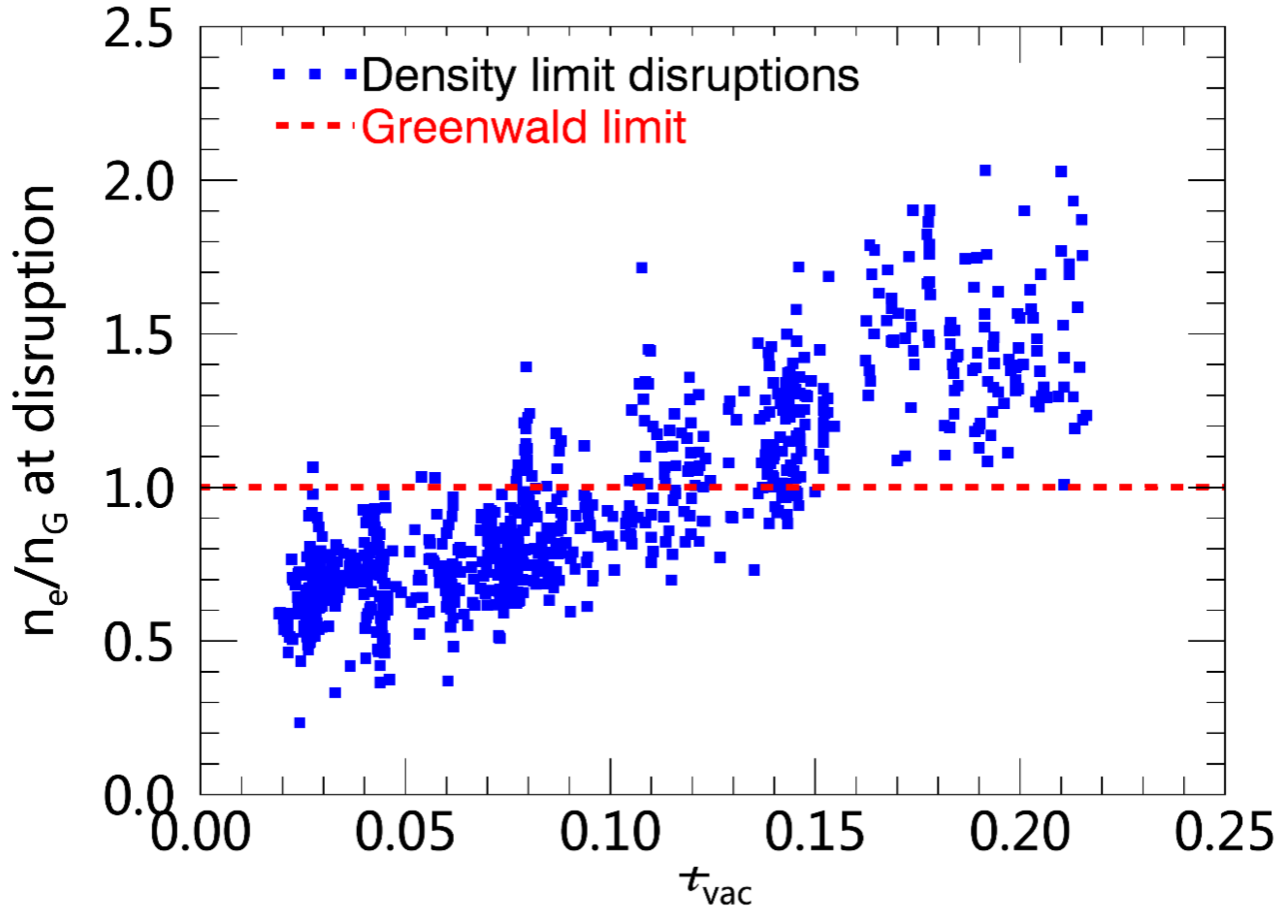

- Ensemble of over 800 disrupting plasmas
- $n_G = \dfrac{I_p}{S_{poloidal}}$
  - $S_{poloidal}$: toroidal averaged poloidal cross section area from reconstructions

Disruptions at high vacuum transform only observed with very peaked current profiles

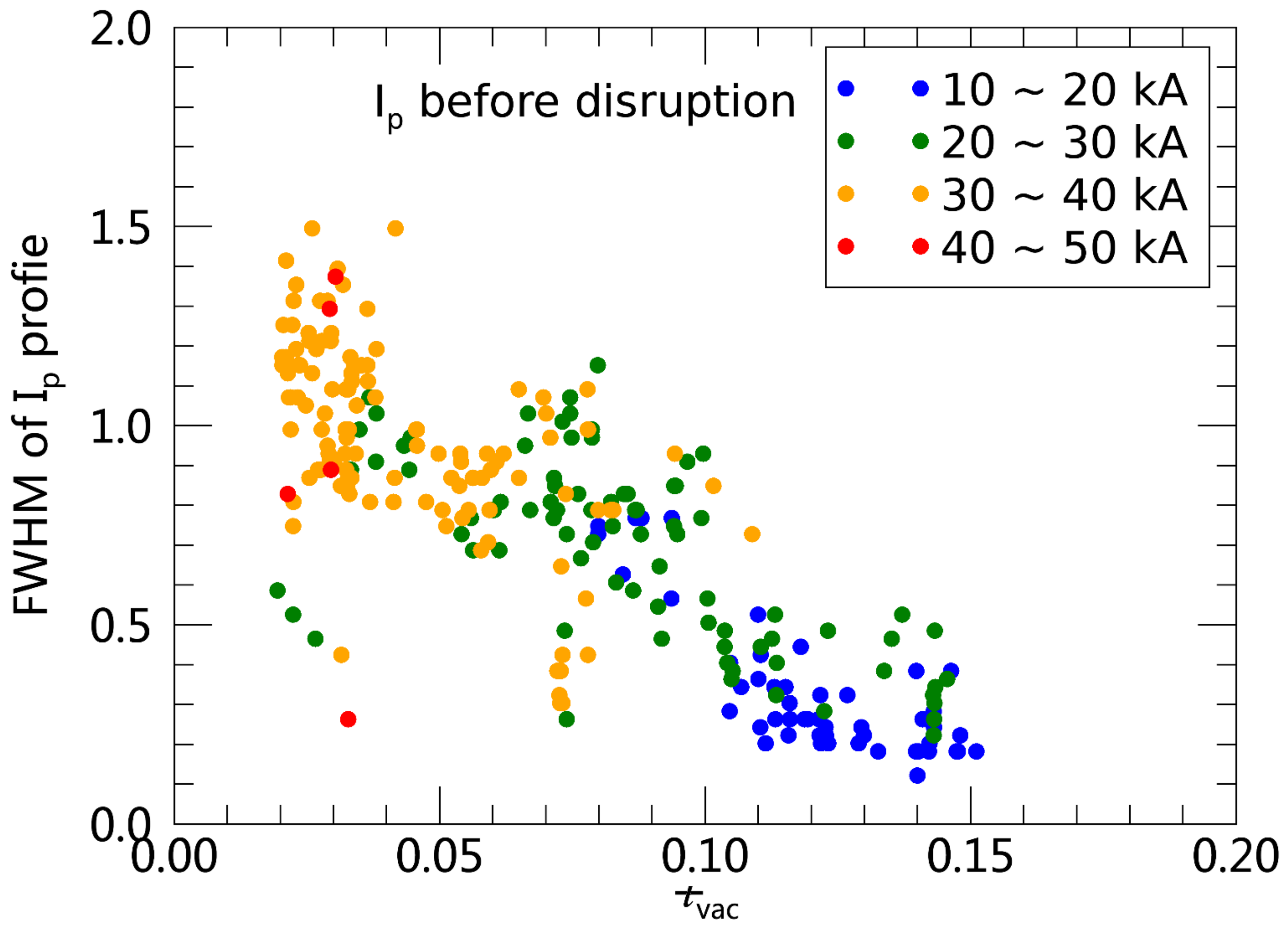

3D equilibrium reconstruction enables further density limit studies by quantifying profile evolution

- Reconstructions show evidence of rapid current profile peaking just prior to the disruption similar to standard tokamak phenomenology
- Addition of 3D stellarator fields flattens both current and q profiles, stabilizing the plasma

3D equilibrium reconstruction enables further density limit studies by quantifying profile evolution

- Reconstructions show evidence of rapid current profile peaking just prior to the disruption similar to standard tokamak phenomenology
- Addition of 3D stellarator fields flattens both current and q profiles, stabilizing the plasma
- Future work will also investigate:
  - Peaking of density profile prior to disruption
  - Possibility of global radiative instability
  - Thermally unstable magnetic islands

Summary

- 3D equilibrium reconstruction is essential for understanding intrinsic 3D confinement in non-axisymmetric plasmas
- With addition of SXR emissivity measurements, V3FIT produces more accurate reconstructions of the core of the plasma
- Density limit disruption in CTH shows tokamak-like signatures
- Density limit disruptions systematically influenced by imposed external transform, with a more detailed physics understanding subject to future work

Back up

Major results

1. With addition of SXR emission measurements, V3FIT produces more accurate reconstructions of the core plasma compared to using magnetics alone
2. Density limit disruptions in CTH show tokamak-like signatures
3. CTH can operate beyond Greenwald density limit with imposed 3D fields
4. Addition of 3D stellarator fields flatten both current and q profiles, providing stabilizing effects

Magnetic signal consists of contributions from plasma current, external coil currents, and eddy currents

$$S^{plasma} = S^{total} - S^{ext} - S^{eddy}$$

- S^{plasma}: signal from plasma current
- S^{ext}: signal from external coil currents
- S^{eddy}: contribution from eddy currents

Accurate modeling of the position and orientation of magnetic diagnostics is crucial for V3FIT reconstructions

$$S^{ext} = \sum_i M_i^{ext} I_i^{ext}$$

- M_i^{ext} are mutual inductances (response functions) between diagnostics and external coils

Accurate modeling of the position and orientation of magnetic diagnostics is crucial for V3FIT reconstructions

$$S^{ext} = \sum_i M_i^{ext} I_i^{ext}$$

- M_i^{ext} are mutual inductances (response functions) between diagnostics and external coils
- Position and orientation optimized using experimental calibration

$$\delta^2 = \sum_{i,j} \left(\frac{M_{ij}^{Model} - M_{ij}^{Exp}}{\Delta M_{ij}^{Exp}} \right)^2$$

Two eddy current sources have been accounted for in V3FIT

- OH transformer and plasma current drive eddy currents
  - Eddy currents induced in vacuum vessel and helical coil frame
- Eddy current modeling
  1. Vacuum vessel
     - 24 toroidal current filaments[6]
  2. Helical coil frame
     - Geometrically modeled as saddle coil

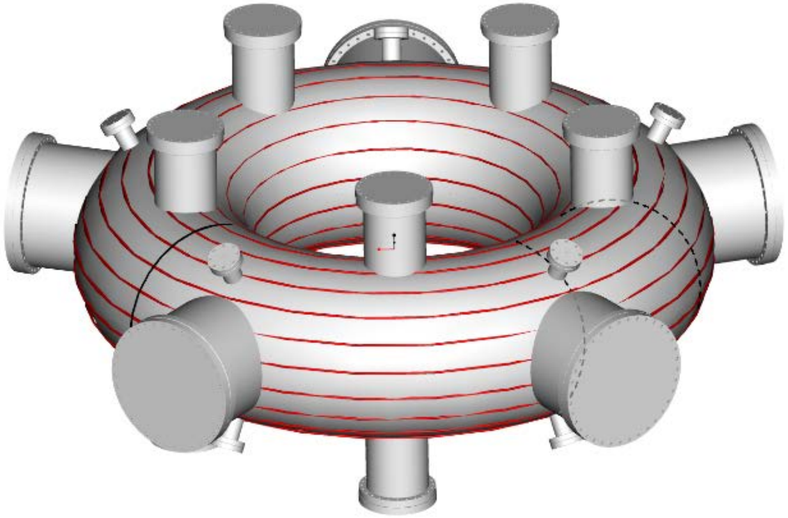

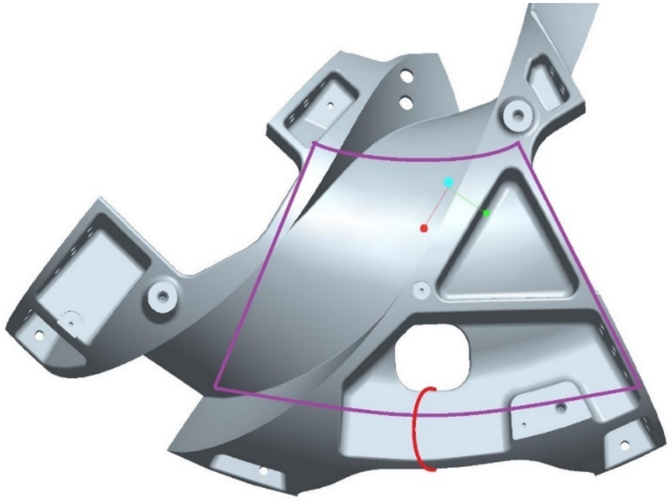

[6] James Bialek *et al.*, Physics of Plasmas, 2001

Simulated signals from reconstructed equilibrium match experimental measurements

16-segment Rogowski

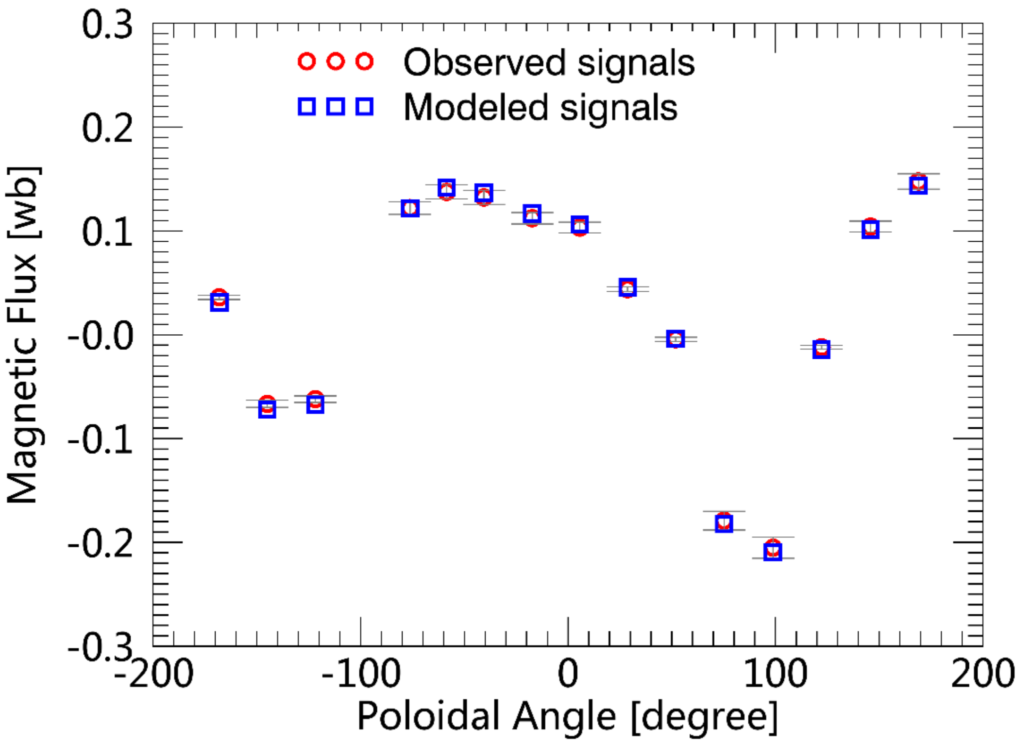

Saddle coils

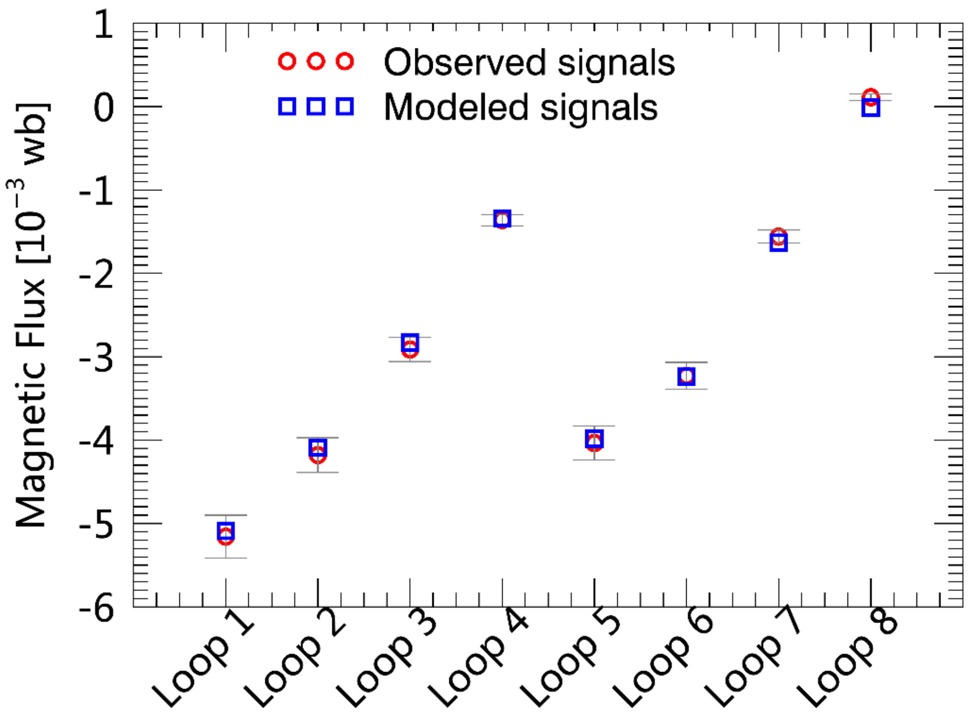

V3FIT successfully employed to reconstruct many different magnetic configurations

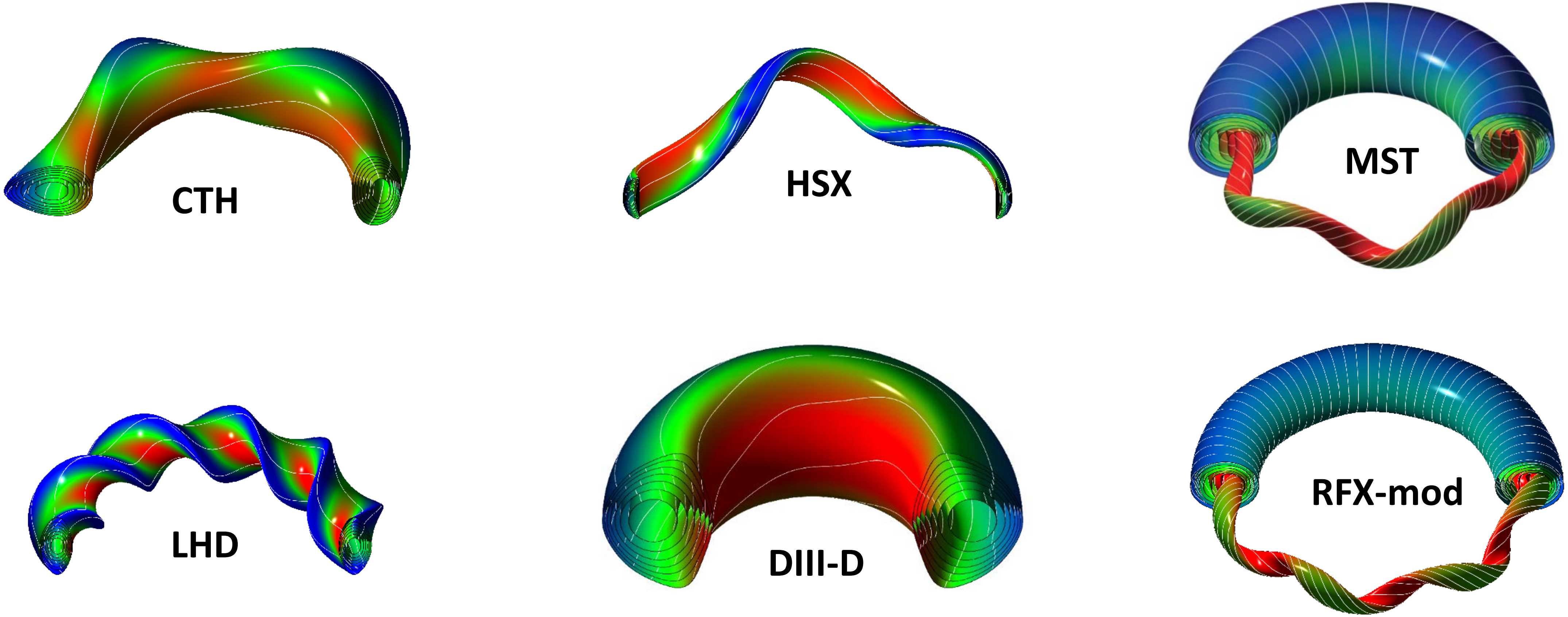

[6] J.D. Hanson *et al.*, Nucl. Fusion, 2013

V3FIT Algorithm (1)

- Minimize deviation between observed and model signal

$$\chi^2(\mathbf{p}) \equiv \sum_i \left(\frac{S_i^O(\mathbf{d},\mathbf{p}) - S_i^m(\mathbf{p})}{\sigma_i}\right)^2$$

$$\mathbf{p}$$

  - Minimize $\chi^2(\mathbf{p})$. Parameters $\mathbf{p}$, observed signals $S_i^O(\mathbf{d},\mathbf{p})$
  - Model-computed signals $S_i^m(\mathbf{d},\mathbf{p})$, uncertainties in signals σ_i
- V3FIT uses Quasi-Newton algorithm for new parameters

$$\mathbf{A}^T \cdot \mathbf{A} \cdot \delta\mathbf{a} = -\mathbf{A}^T \cdot \mathbf{e}$$

  - Jacobian (normalized) $A_{ij} = \frac{\pi_j}{\sigma_i}\left(\frac{\partial S_i^o}{\partial p_j} - \frac{\partial S_i^m}{\partial p_j}\right)$ $\chi^2(\mathbf{p}) = \mathbf{e} \cdot \mathbf{e}$
  - Error vector $e_i = (S_i^O(\mathbf{d},\mathbf{p}) - S_i^m(\mathbf{p}))/\sigma_i$ $\mathbf{A} = \nabla_{\mathbf{a}}\mathbf{e}$
  - Normalized Parameters $a_j = p_j/\pi_j$

V3FIT Algorithm (2)

- Jacobian Calculation
  - Finite difference approximation, $J_{ij} \approx \Delta S_i / \Delta p_j$
  - Small Δp in parameter space – VMEC converges rapidly
  - Need moderate accuracy in S_i^m
  - Needs well-converged VMEC
  - Does not need high radial resolution – improves speed
  - Use SVD on Jacobian to help avoid large steps in parameter space
- Posterior Sigmas – Confidence Limits on Parameters
  - Assume uncorrelated signals – diagonal signal covariance matrix
  - Parameter covariance matrix (also called posterior covariance)

$$\mathbf{C}_p = (\mathbf{J}^T \cdot \mathbf{C}^{-1} \cdot \mathbf{J})^{-1} \qquad C_{ij} = \sigma_i^2 \delta_{ij}$$

  - Confidence limit on parameter value - Measures how accurately these signals determine the jth reconstruction parameter. $\sigma_{pj} = \sqrt{(\mathbf{C}_p)_{jj}}$

Signal Effectiveness

- Proposed measure of the effectiveness of a signal:

$$R_{ij} = \frac{\partial \ln \sigma_{pj}}{\partial \ln \sigma_i} = \frac{\sigma_i}{\sigma_{pj}} \frac{\partial \sigma_{pj}}{\partial \sigma_i}$$

  - Logarithmic derivative of the jth posterior parameter σ_p with respect to the ith signal σ
  - How much will the jth posterior σ_p improve if the noise level on the ith signal is reduced?
- R_{ji} is dimensionless, non-negative and normalized $\sum_i R_{ji} = 1$
- Essentially indicates how effective an individual signals is in determining a particular set of parameters

Saddle coils installed in positions optimized to be most sensitive to changes in the current profile

Saddle coil signal effectiveness contour for the current profile width

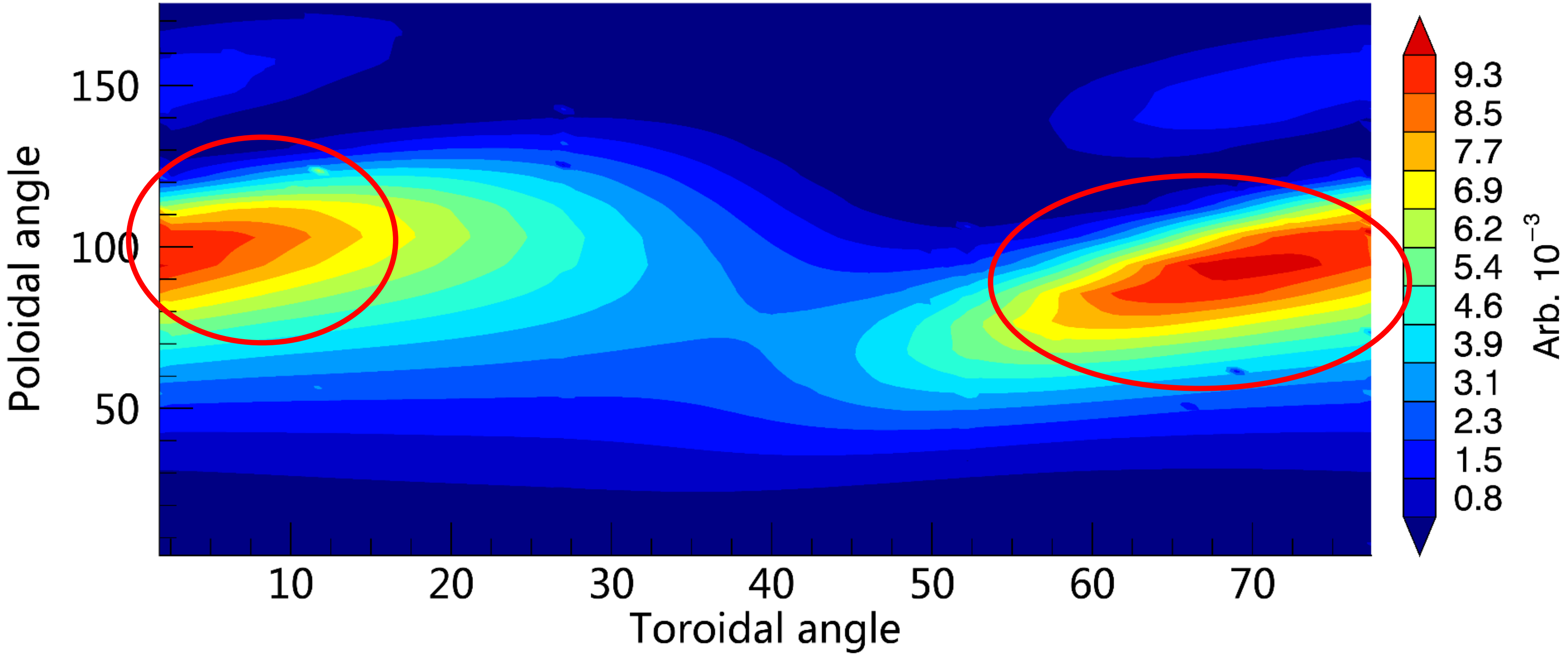

- $\text{Signal effectiveness} = \dfrac{\text{change in parameter}}{\text{change in signal}}$

Magnetic diagnostics installed on the inner wall, positions measured by CMM

Saddle coils wound in tubes and supported by stainless steel frames

Rogowski coils installed on inner wall of vacuum vessel

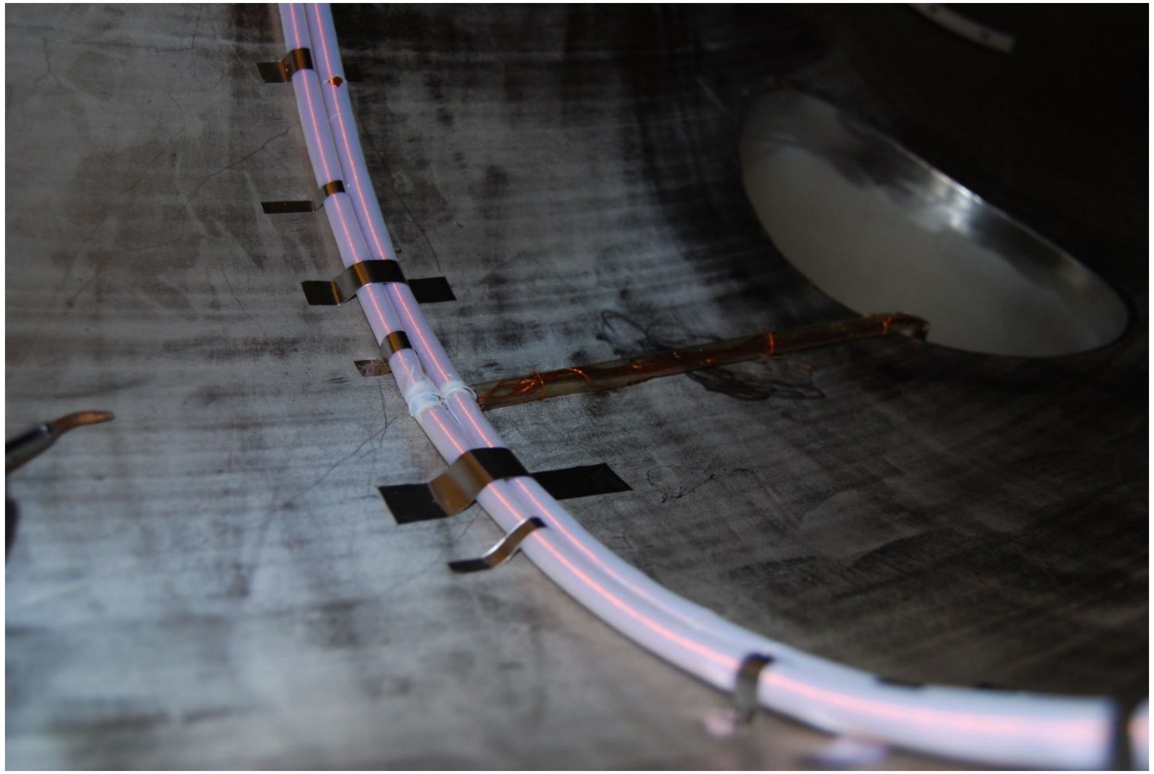

Accurate modeling of the position and orientation of magnetic diagnostics is crucial for V3FIT reconstructions

$$S^{ext} = \sum_i M_i^{ext} I_i^{ext}$$

- M_i^{ext} are mutual inductances (response functions) between diagnostics and external coils
- Position and orientation optimized using experimental calibration

$$\delta^2 = \sum_{i,j} \left(\frac{M_{ij}^{Model} - M_{ij}^{Exp}}{\Delta M_{ij}^{Exp}} \right)^2$$

Mutual inductances from optimized geometric model match experimental calibrated values

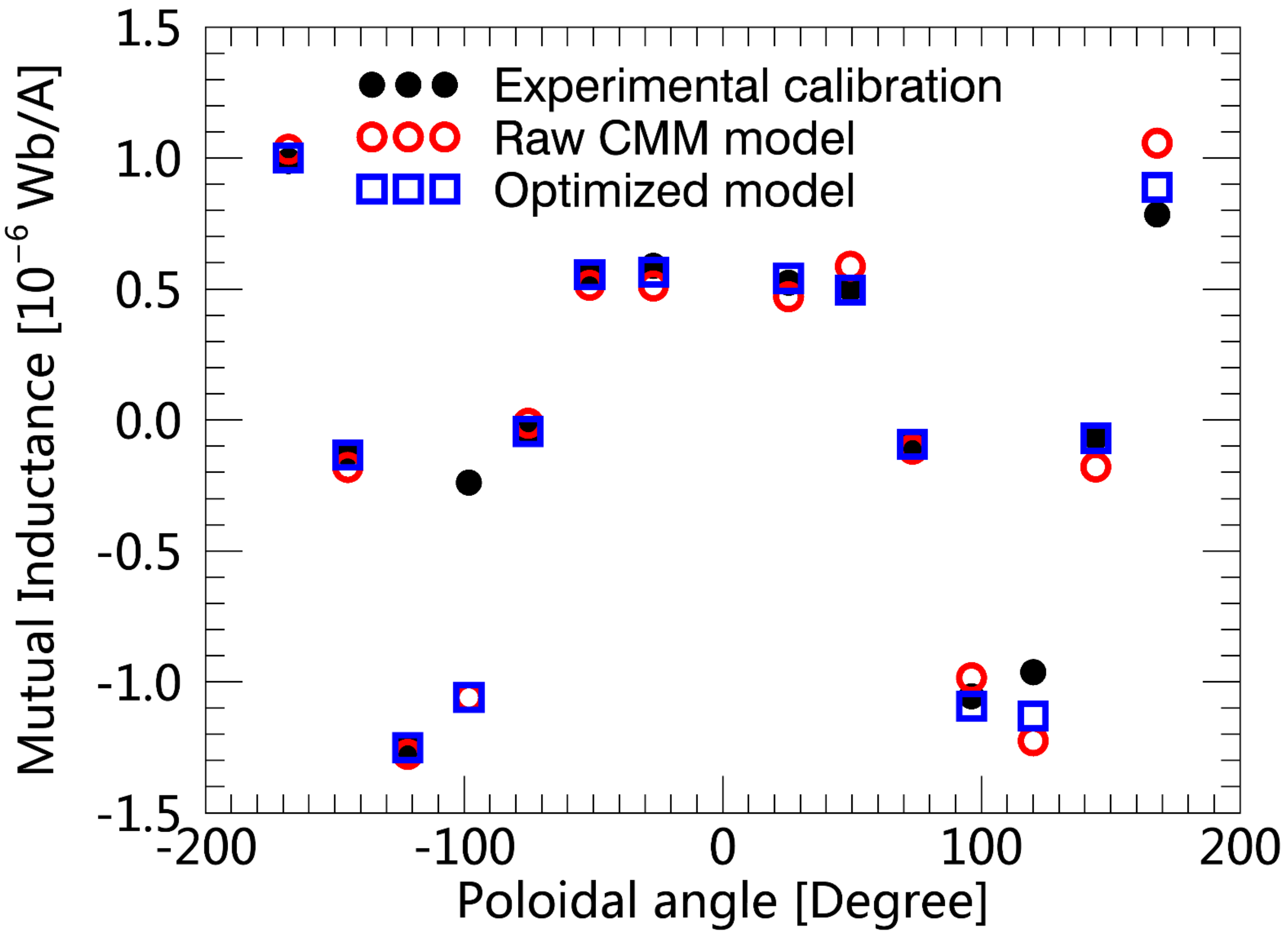

Eddy current signals represent only minor corrections to the diagnostic signals

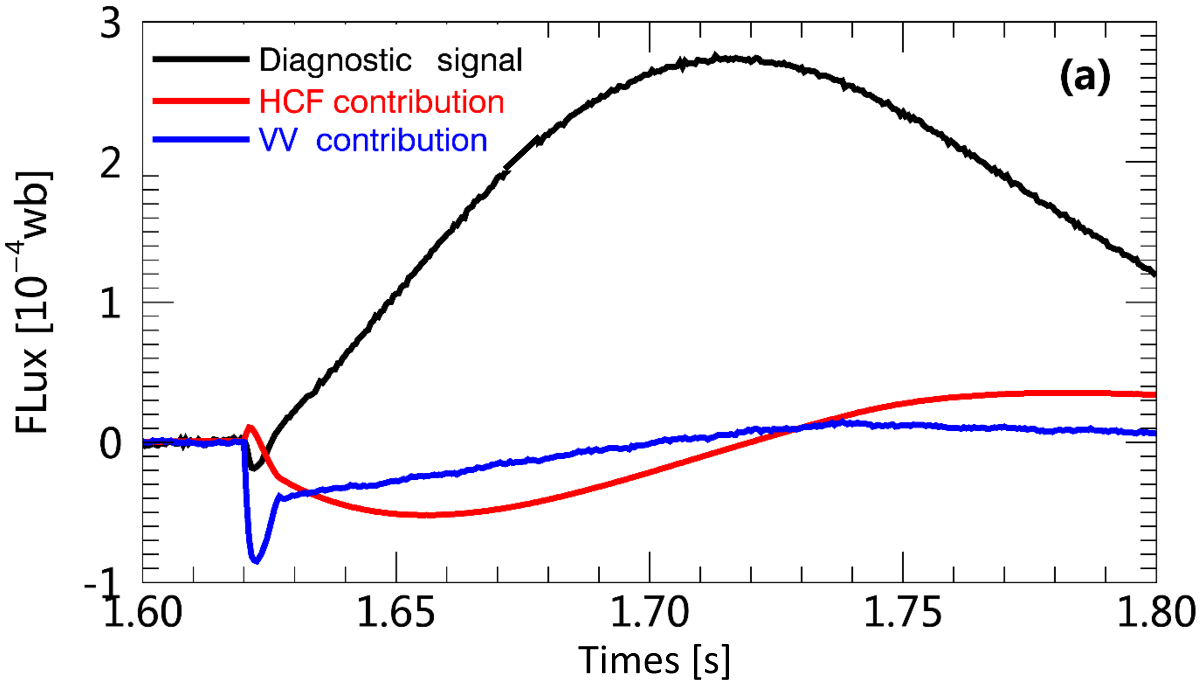

Without plasma current

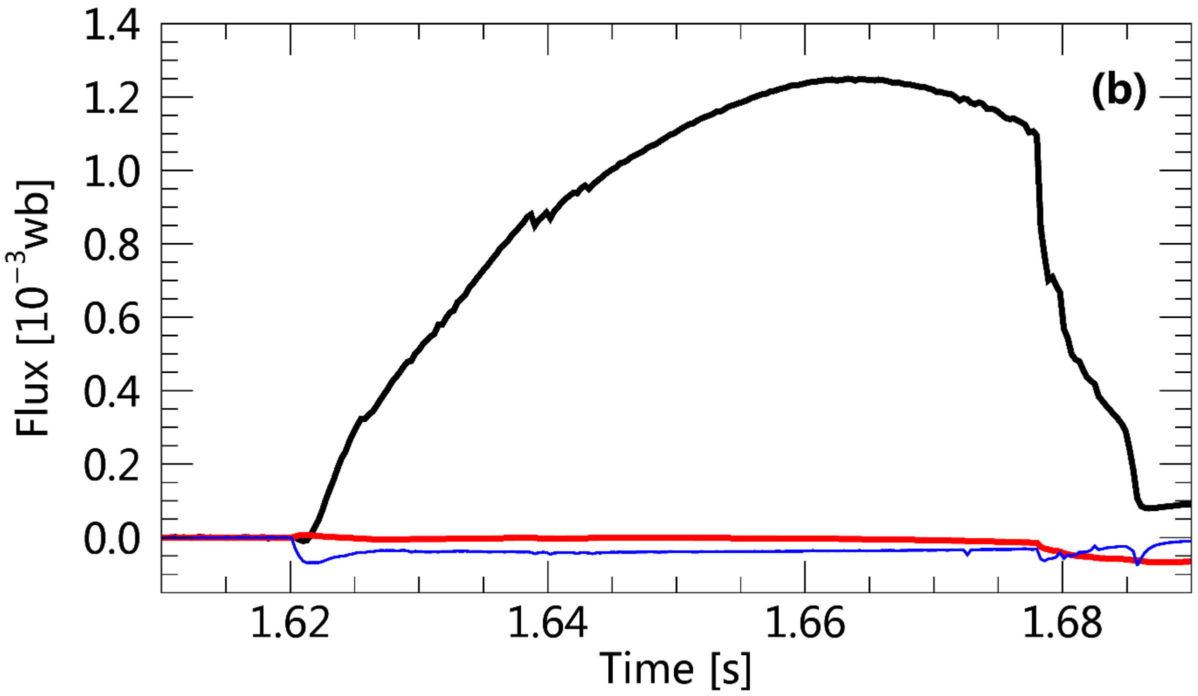

With plasma current

Two power model employed for both current and pressure profiles

- A two power model is employed for pressure and current density profiles
  - $A(s) = A_o(1 - s^{\alpha})^{\beta}$
- The current profile parametrization is based on a single fitting parameter α:
  - $I'(s) = I_o(1 - s^{\alpha})^6$
- A flat profile is assumed for pressure
  - $P(s) = P_o(1 - s^{10})^2$

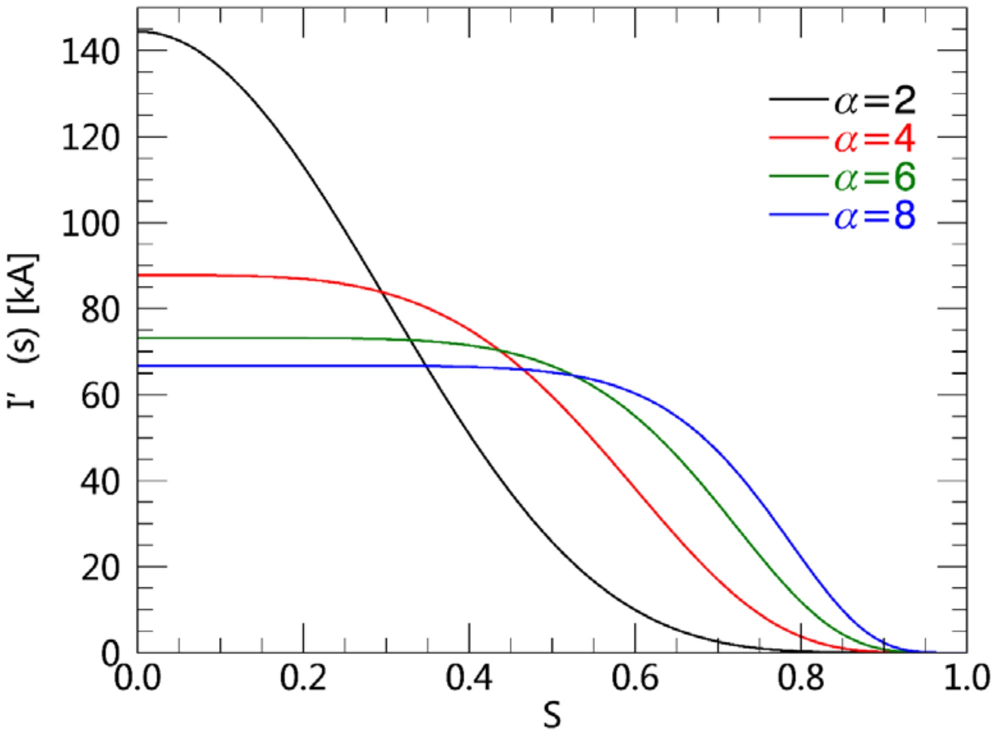

A flat pressure profile is assumed

- Central electron temperature (< 150 eV) is obtained with SXR bremsstrahlung spectroscopy
- The three-channel interferometer shows relative flat density profile
- Chordal measurements of the SXR emission also shows relative flat electron temperature profile
- A broad pressure profile is assumed

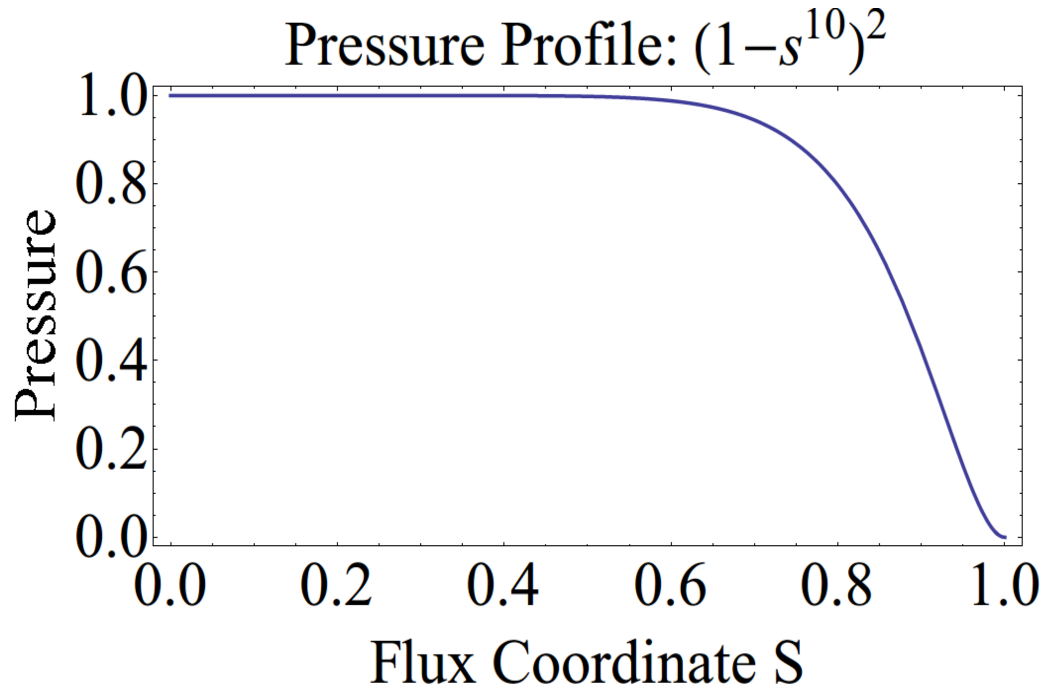

Example of a whole shot reconstruction

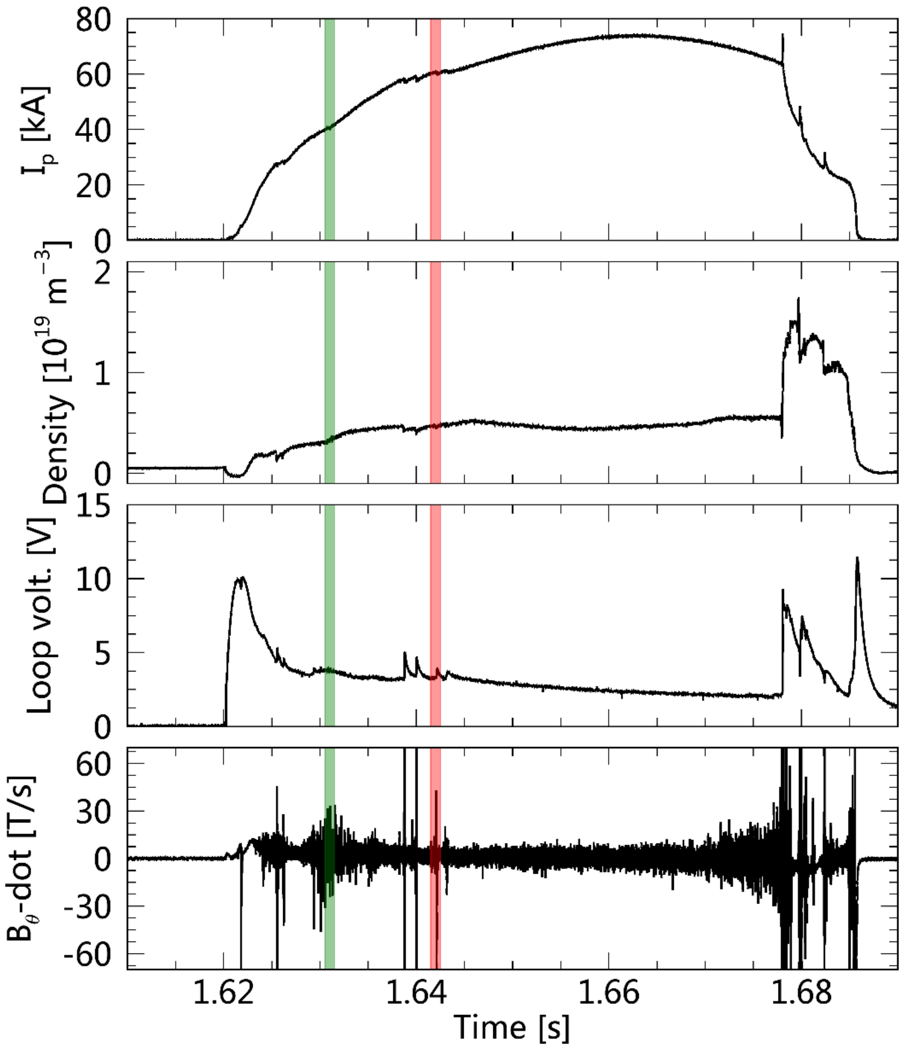

Reconstructions provide time-dependent equilibrium parameters

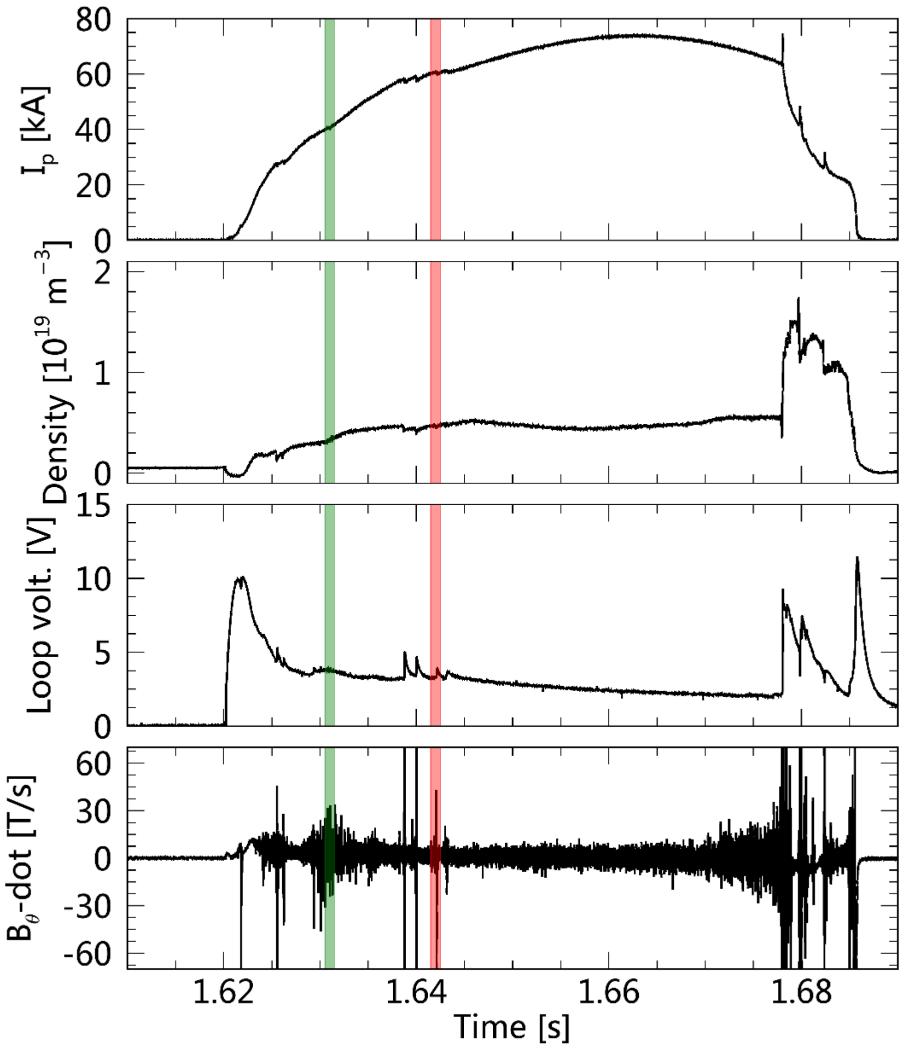

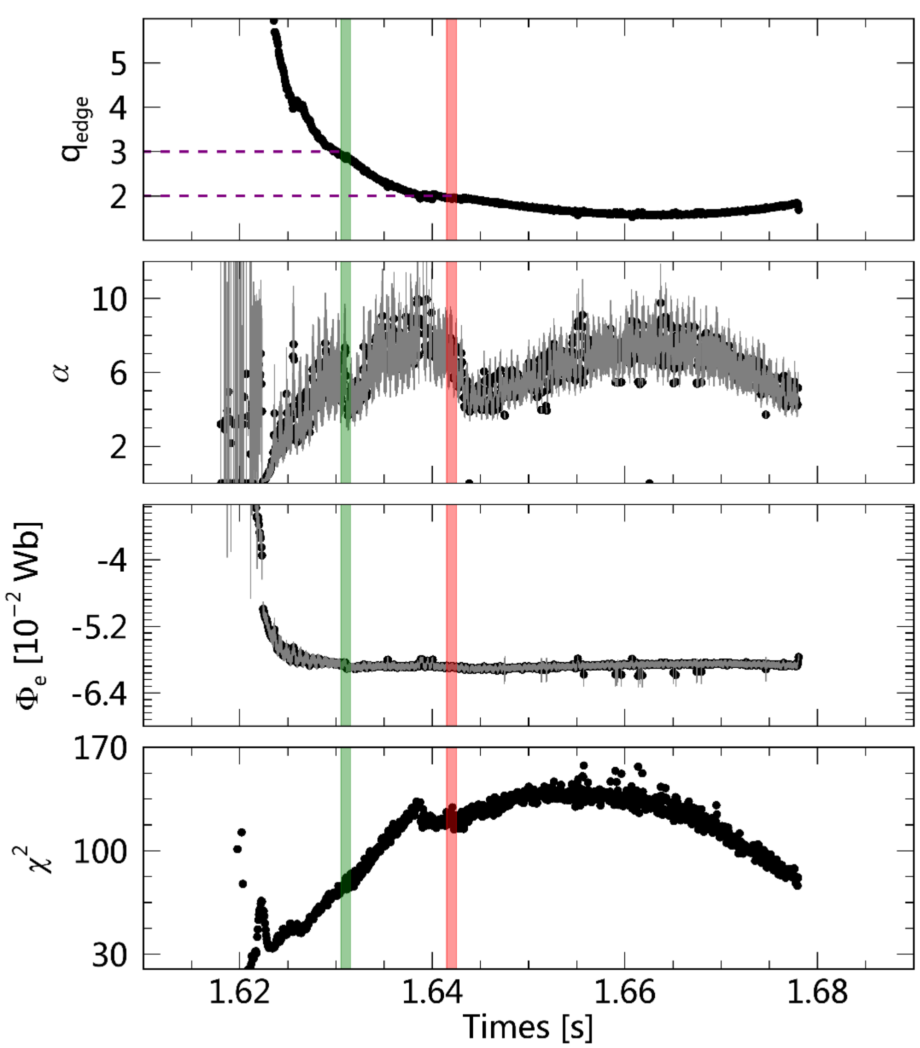

Plasma geometry is more rigid at the half period of CTH

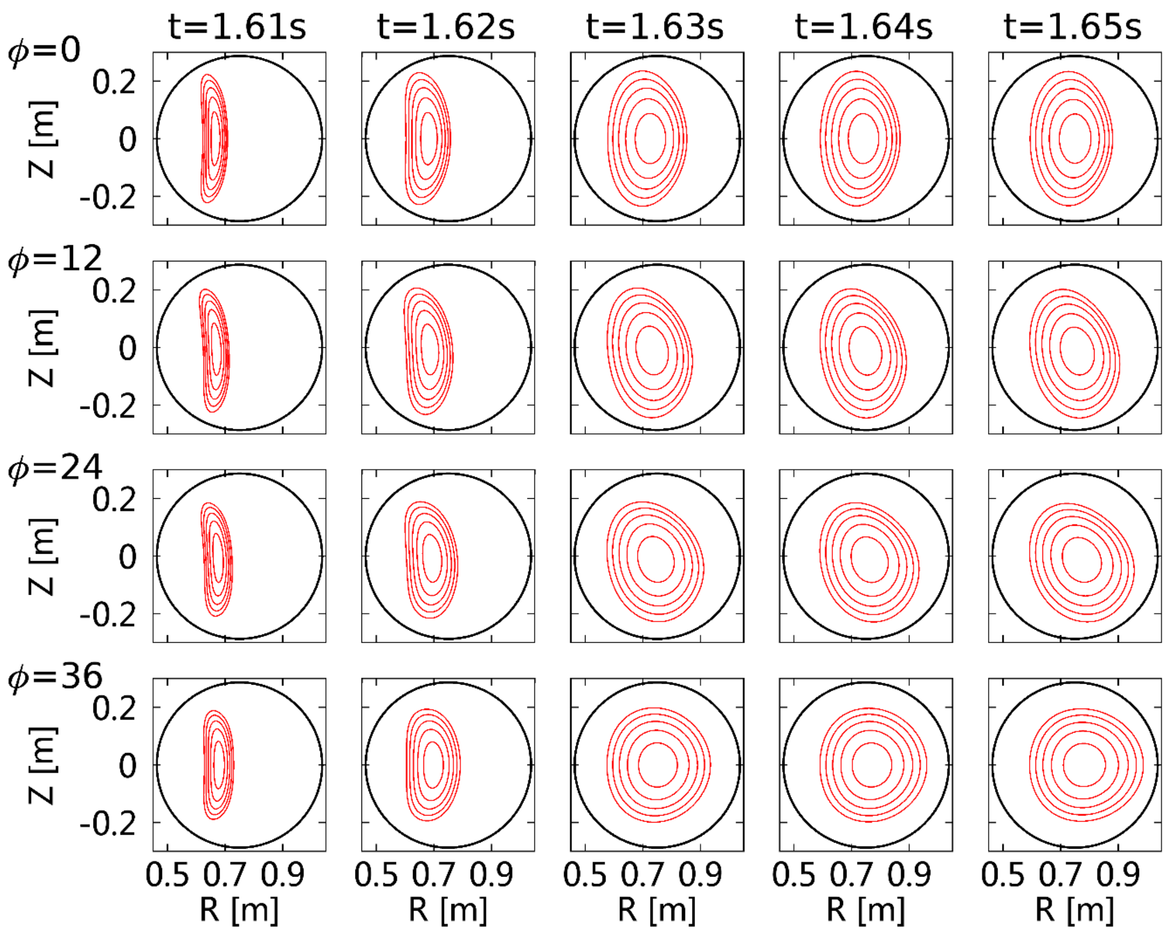

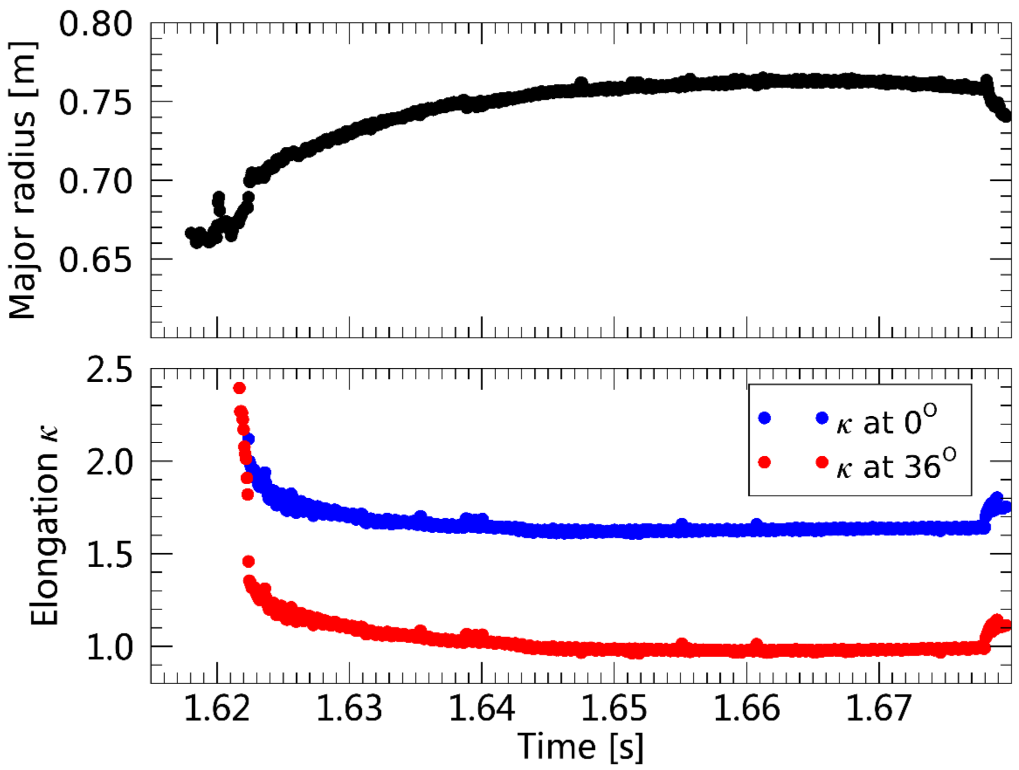

SXR measurements are far more sensitive to changes of current profile than external magnetic measurements

Signal effectiveness with respect to current profile parameter (averaged over 144 different plasmas)

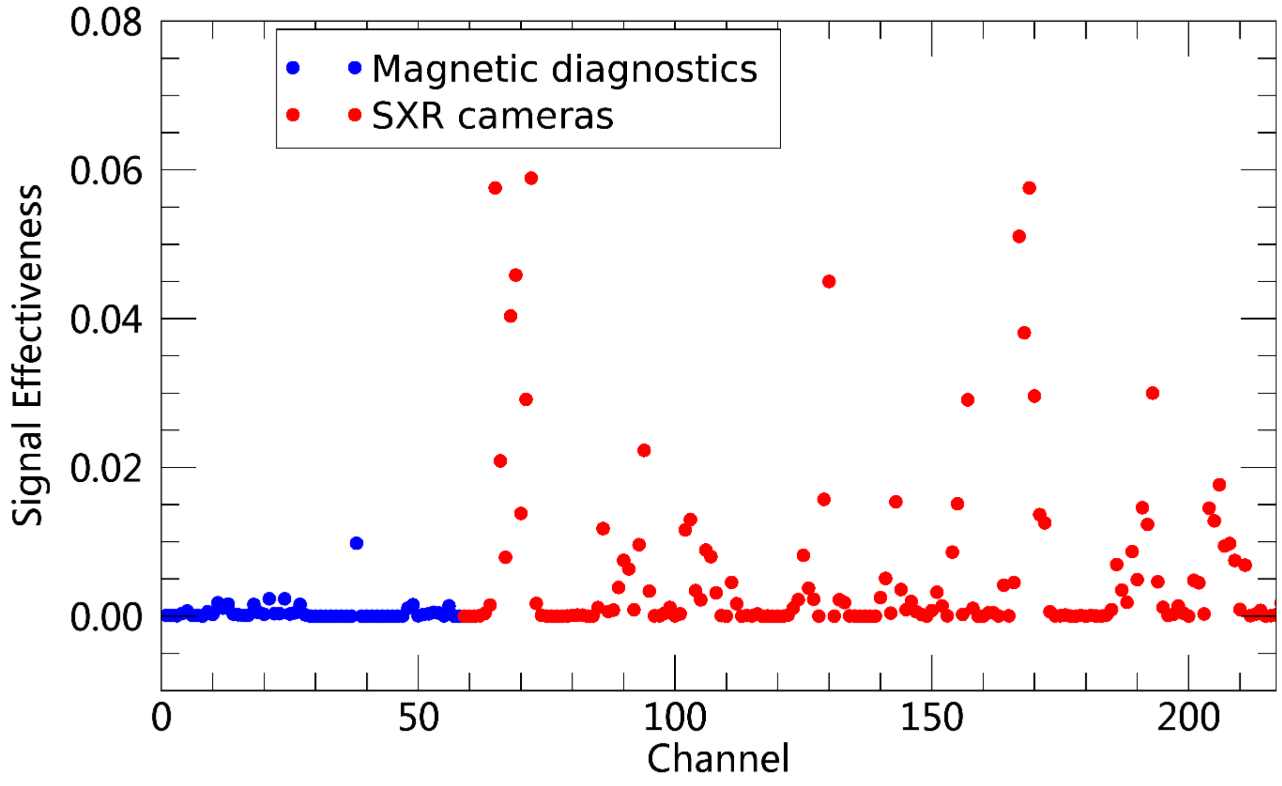

Signal effectiveness of all SXR cameras

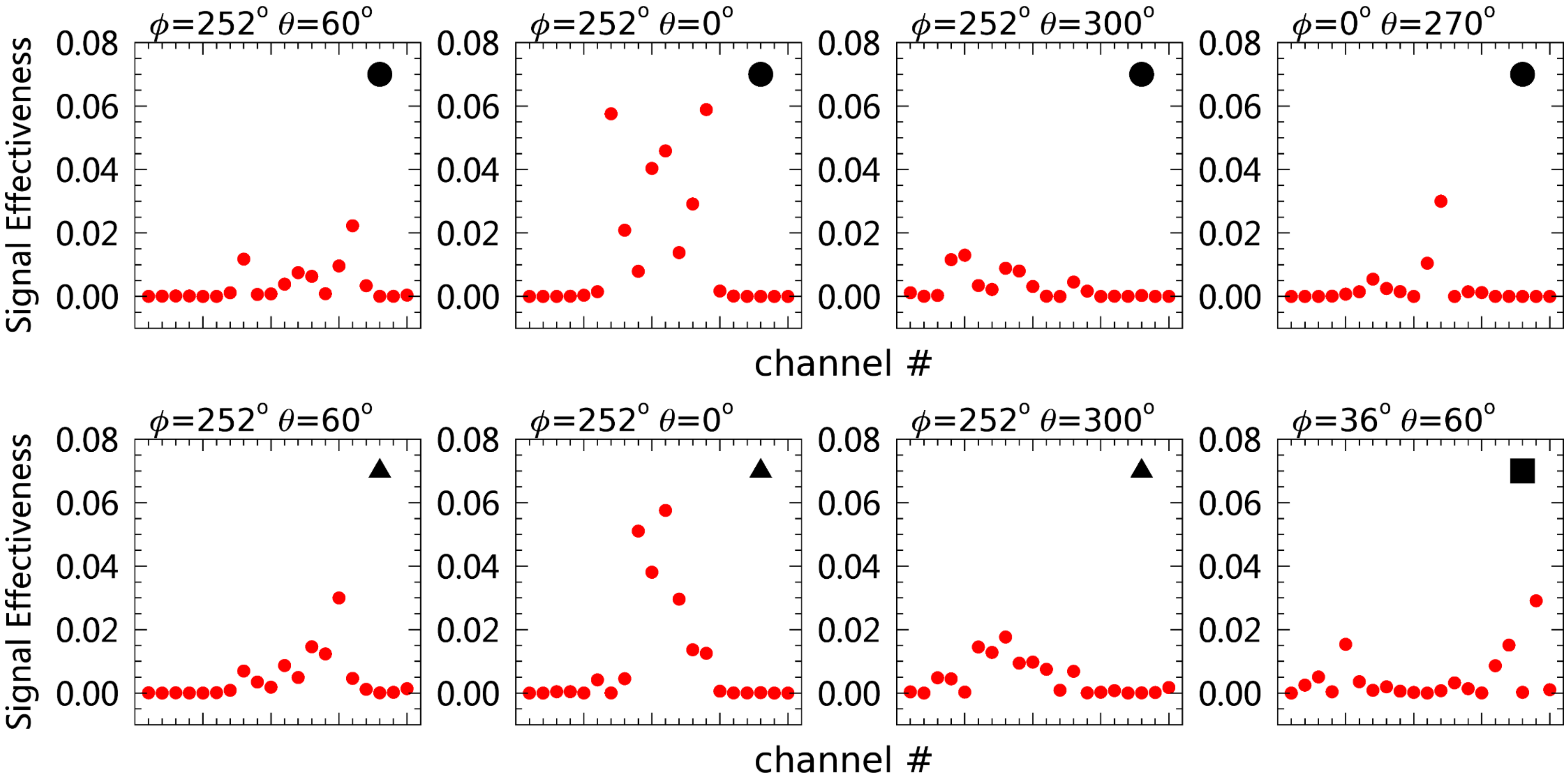

Reconstructed q_{edge} values are consistent for all reconstruction methods

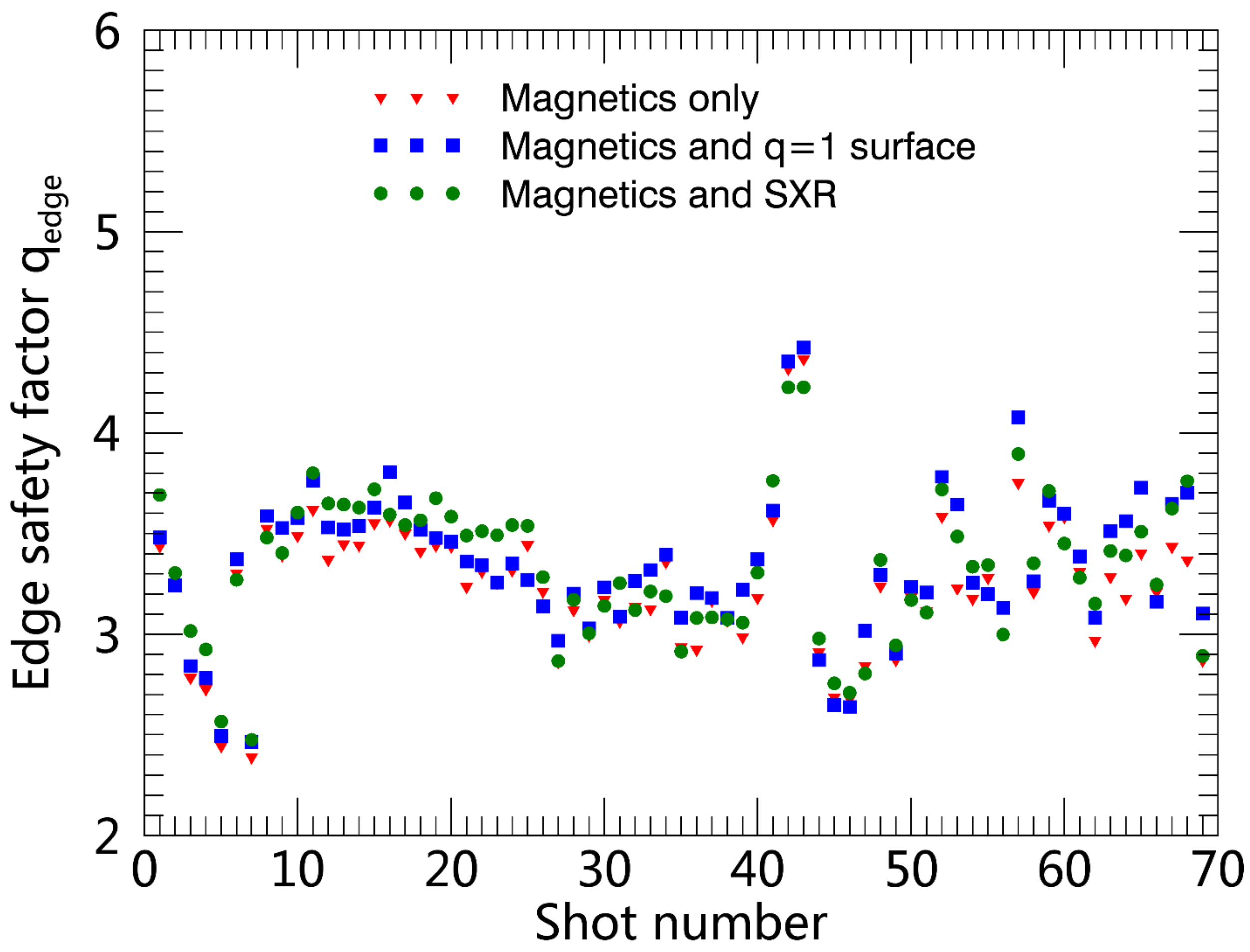

Density at disruption observed to be independent of plasma current evolution

- Different programmed loop voltages
- Disruption occurrence correlates with plasma current and density as in tokamaks

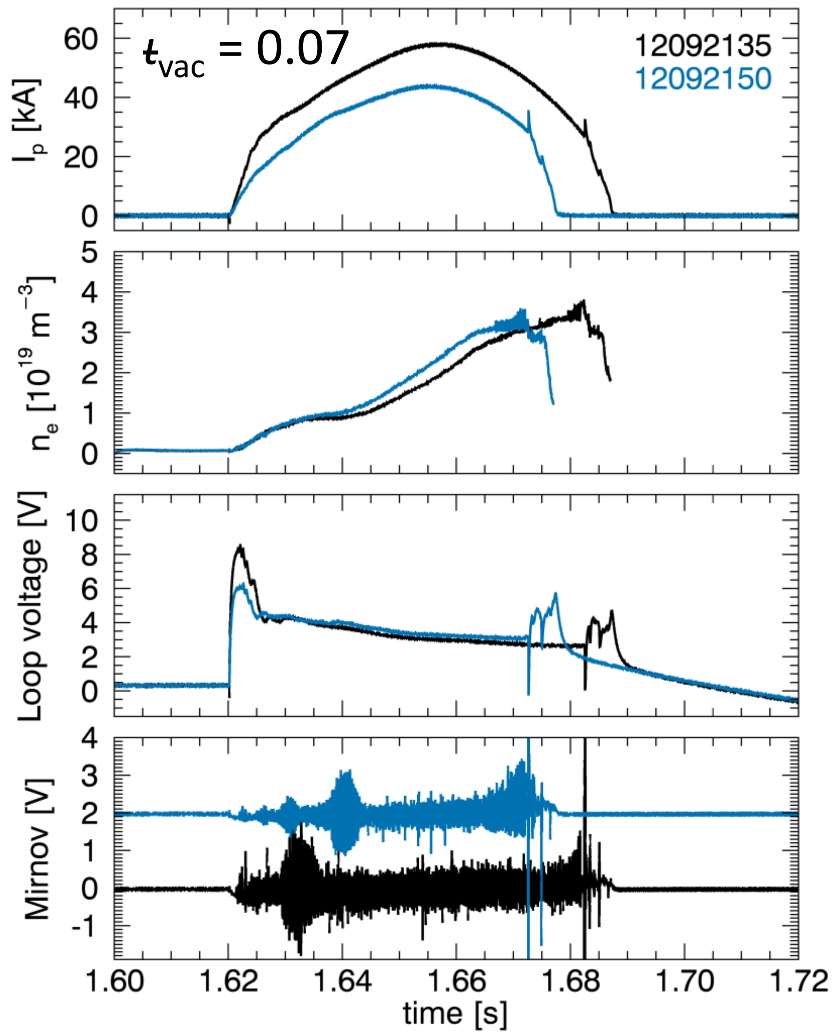

Addition of external vacuum transform elevates the stability parameter Δ' associated with the 2/1 tearing mode

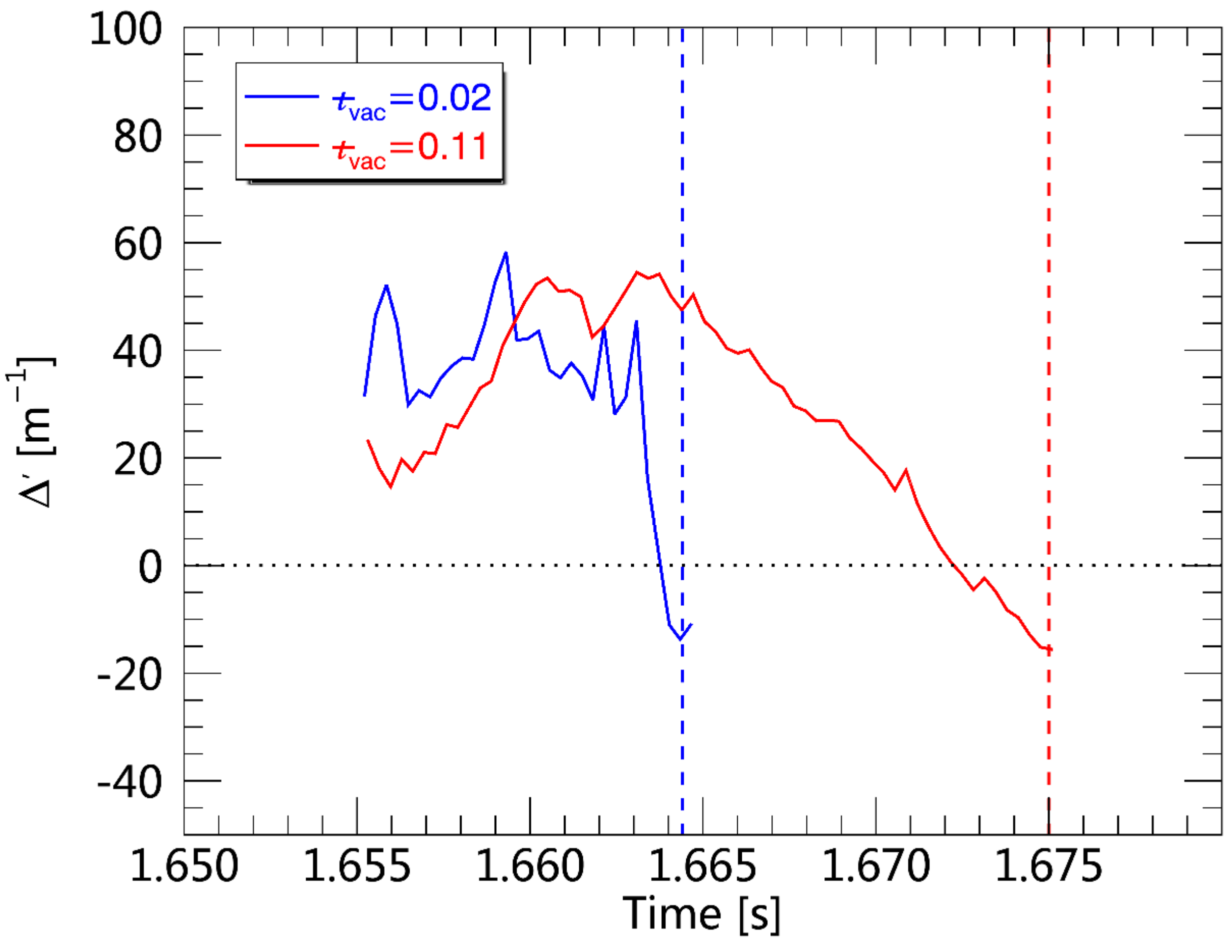

- Stability parameter Δ' decreases and passes zero before disruption
- Additional vacuum transform elevates the value of Δ'

Density at disruption scales with the plasma current and vacuum transform

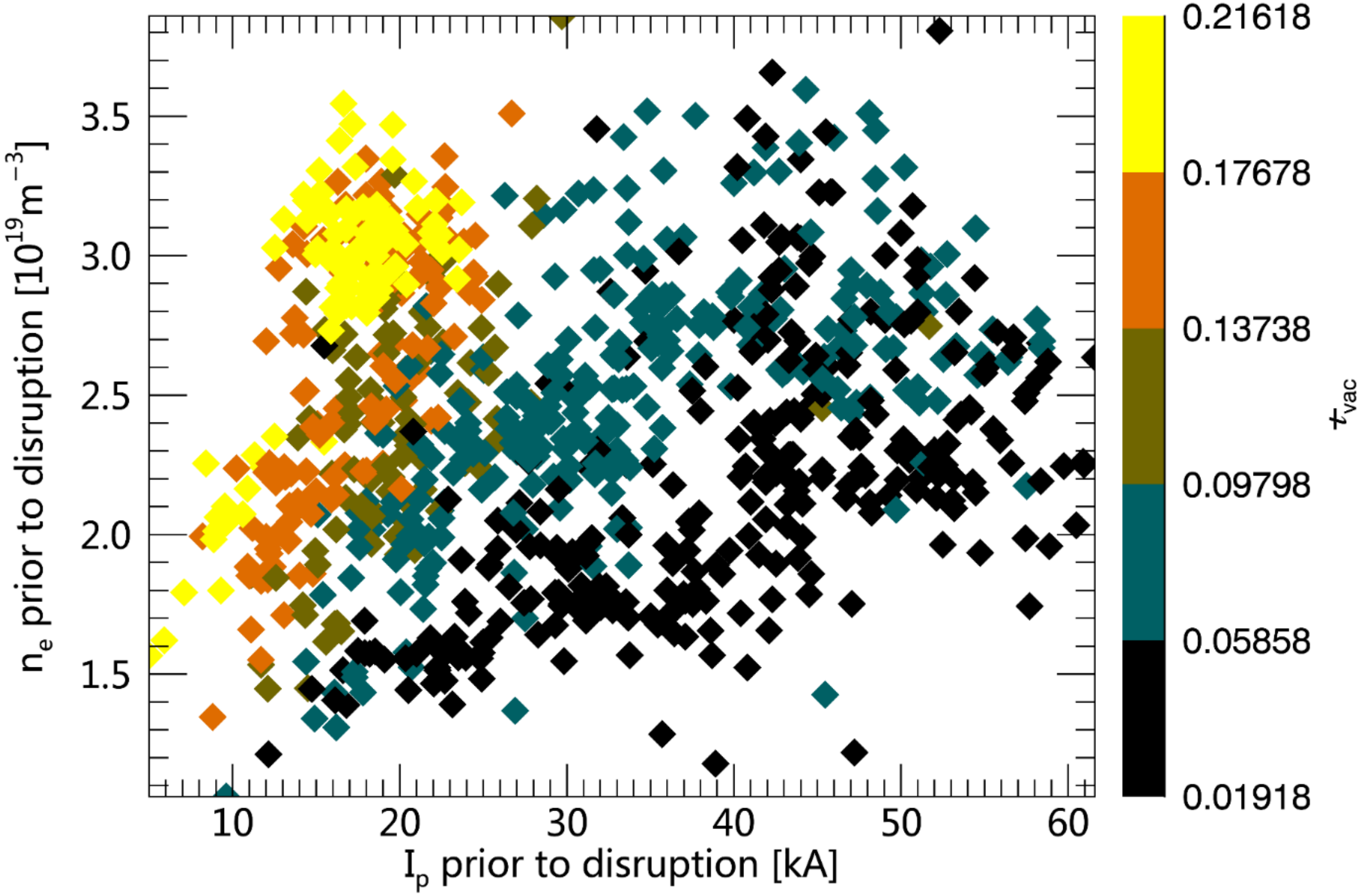

Deuterium plasma shows improved performance in CTH

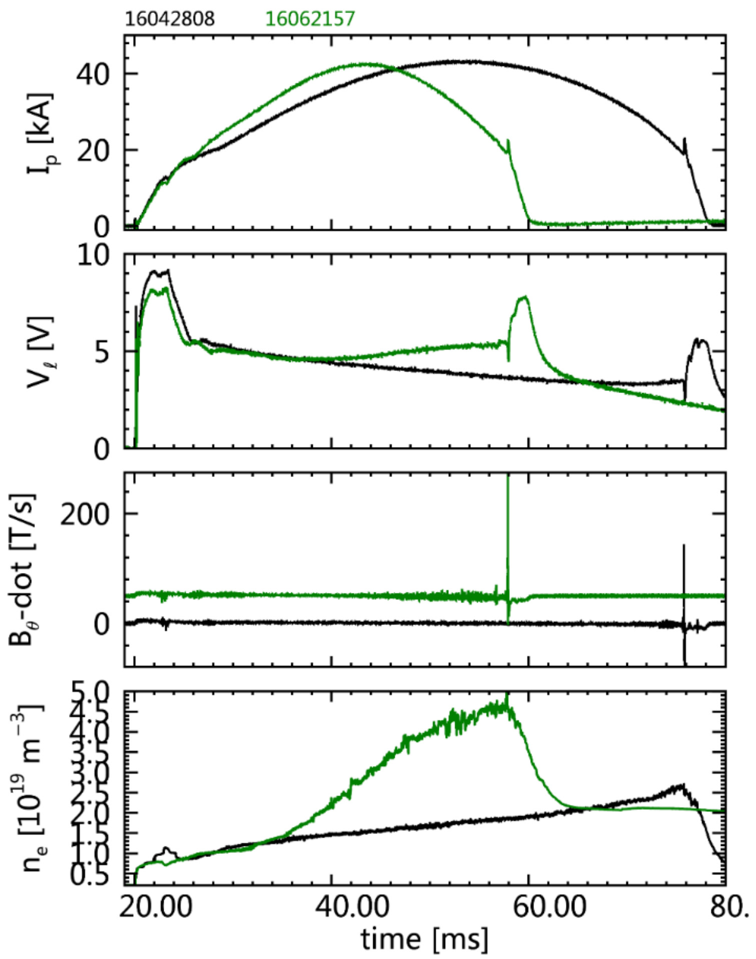

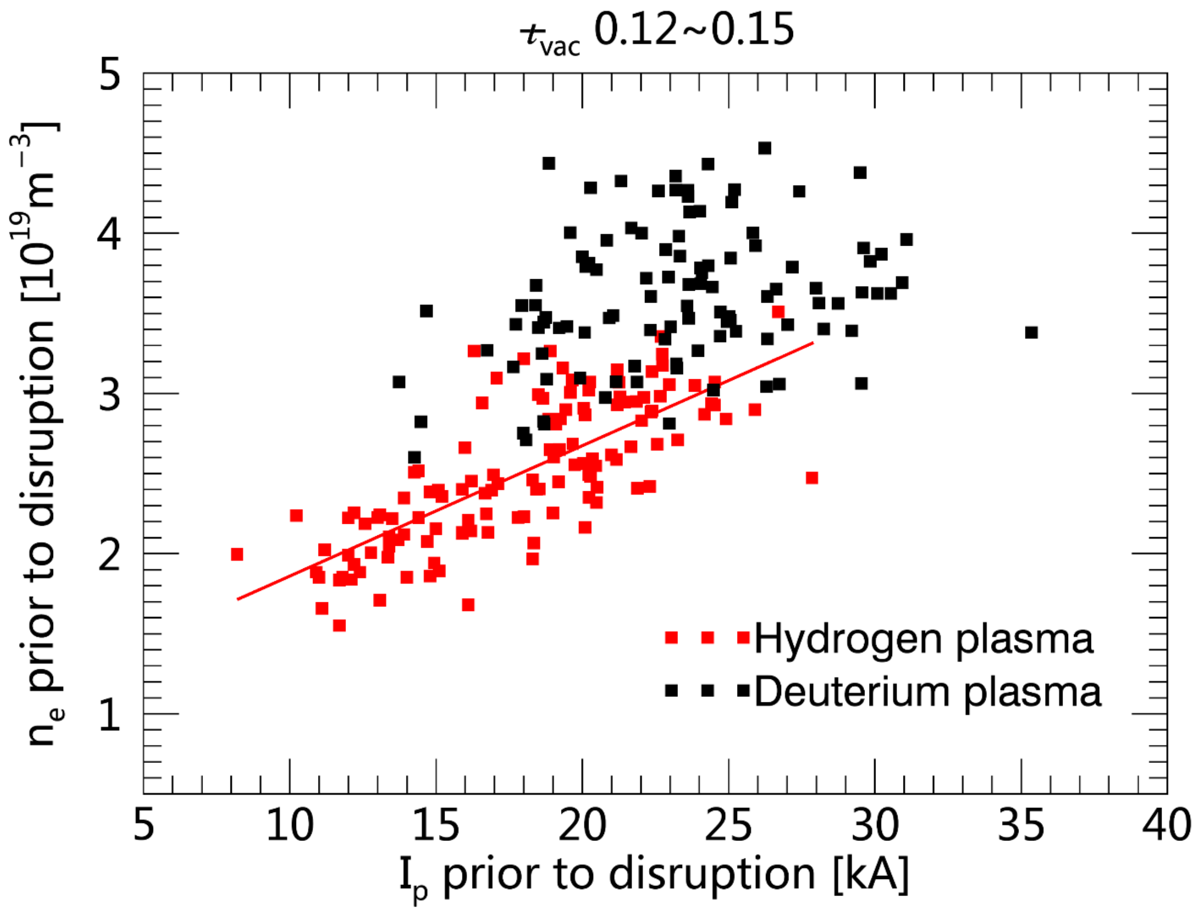

More physics to investigate

- Limited current profile knowledge makes it hard to determine current gradient near edge for instability calculation
  - External magnetics only measure the total current
  - SXR measurements fit current distribution near center
- Peaking of density profile prior to disruption?
  - More channels for interferometer
- Present of rotating islands near edge?
  - Tomography of SXR and Bolometer measurements
- Evidence of radiative instability?
  - Bolometer to measure the total radiated power